Precambrian Research 397 (2023) 107166

Contents lists available at ScienceDirect

Precambrian Research

journal homepage: www.elsevier.com/locate/precamres

Geochronology and chemostratigraphy of the 2.47–1.96 Ga rift-related volcano-sedimentary succession in the Karasjok Greenstone Belt, northern Norway, and its regional correlation within the Fennoscandian Shield

Harald Hansen [a,*], Trond Slagstad [b], Steffen G. Bergh [a], Andrey Bekker [c,d]

[a] UiT The Arctic University of Norway, N-9037 Tromsø, Norway
[b] Geological Survey of Norway, N-7491 Trondheim, Norway
[c] University of California, Riverside, CA 92521, USA
[d] University of Johannesburg, South Africa

ARTICLE INFO

Keywords:
Fennoscandia
Paleoproterozoic
U-Pb geochronology
Magmatism
Isotope geochemistry
Lomagundi carbon isotope excursion

ABSTRACT

New geochronological data for the amphibolite-facies volcano-sedimentary Karasjok Greenstone Belt in northwestern Fennoscandia bracket its age between 2.47 and 1.96 Ga. The volcano-sedimentary units were deposited on the 3005 ± 24 to 2776 ± 69 Ma crystalline basement rocks of the Jergul Gneiss Complex. The lowermost Vuomegielas Formation contains rhyodacites dated at 2469 ± 12 Ma that were deposited in an intracratonic rift setting related to the Matachewan mantle plume event. The overlying Skuvanvárri Formation, correlative with the early *Jatulian* (c. 2.2 Ga) units on the Fennoscandian Shield, consists of siliciclastic sedimentary rocks deposited in coastal deltaic and shallow-marine settings. The overlying *mid-Jatulian* Gollebáiki Formation contains 2151 ± 5 Ma mafic intrusions and tholeiitic basalts related to a rifting event and breakup of the Superia supercraton that resulted in voluminous volcanic and shallow-marine deposits. The Ni-Cu-PGE-mineralized Porsvann intrusion, hosted by the Gollebáiki Formation, yielded an age of 2056 ± 10 Ma, which corresponds with other Ni-Cu-PGE-bearing intrusions on the Fennoscandian Shield. The uppermost Báhkilvárre Formation consists of basalts, komatiites, and andesitic lavas. A synvolcanic gabbro within the komatiites in the lower part of the formation yielded an age of 1984 ± 16 Ma. Andesites in the upper part of the same formation were dated at 1961 ± 1 Ma. They represent the final Paleoproterozoic magmatic event that affected large areas of the Fennoscandian Shield prior to the Lapland-Kola and Svecofennian orogenies. Carbon isotope values for carbonates of the Skuvanvárri and Gollebáiki formations range up to highly positive (+12.4 ‰) values, corresponding to the c. 2.22–2.06 Ga Lomagundi carbon isotope excursion. In contrast, carbonates from the Báhkilvárre Formation do not yield elevated $\delta^{13}C$ values, indicating that it was deposited in the aftermath of the Lomagundi carbon isotope excursion. New geochronologic and chemostratigraphic data for the Karasjok Greenstone Belt support correlation with the early Paleoproterozoic sedimentary successions deposited on the eastern margin of the Superior craton and position the northern-northwestern margin of the Karelia-Kola craton against the eastern margin of the Superior craton between c. 2.5 and 2.05 Ga.

1. Introduction

Early Paleoproterozoic, rift-related supracrustal belts record an important period of the Earth's surface and crustal evolution and the onset of modern plate tectonics.The northeastern part of the Fennoscandian Shield consists of the Archean Kola and Karelia cratons overlain by extensive Paleoproterozoic volcano-sedimentary successions and intruded by contemporaneous igneous rocks. Therefore, this part of the Fennoscandian Shield represents an important archive for studying early rifting, development of continental margins, and orogenic tectonic processes (e.g., Lahtinen and Huhma, 2019; Skyttä et al., 2019).

The Kola and Karelia cratons were part of the Superia supercraton (Bleeker, 2003) that also included the Superior, Wyoming, Hearne, Rae, Kaapvaal, Pilbara, and Zimbabwe cratons (Gumsley et al., 2017; Davey et al., 2020; Davey et al., 2022) until its ultimate breakup at c. 2.06 Ga (Mammone et al., 2022). These cratons share a common magmatic and

* Corresponding author.
E-mail address: Harald.Hansen@uit.no (H. Hansen).

https://doi.org/10.1016/j.precamres.2023.107166
Received 26 January 2023; Received in revised form 21 August 2023; Accepted 24 August 2023
Available online 9 September 2023

tectonic history, including protracted, episodic rifting of the Superia supercraton between c. 2.5 and 2.1 Ga. The position of the Kola and Karelia cratons in the Superia supercraton is still debated; Ernst and Bleeker (2010) placed them along the eastern margin of the Superior craton, while Davey et al. (2020, 2022) preferred to place them against the modern western margin of the Wyoming craton. Regardless, all these reconstructions attach the northern to northwestern margins of the Kola and Karelia cratons to the rest of the Superia supercraton until c. 2.1 Ga. It is thus critical to calibrate the Paleoproterozoic tectonostratigraphic records along the northern margin of Fennoscandia to constrain when rifting events and continental breakup occurred along this cratonic margin.

Significant changes in atmospheric composition during the Paleoproterozoic, as well as carbon isotope excursions in marine carbonate sequences, further require robust and precise geochronological constraints for their temporal calibration. Carbonate sequences, especially those deposited on open continental margins, provide evidence of changing geochemical conditions through time and enable temporal calibration since the early Paleoproterozoic seawater experienced multiple, global positive and negative carbon isotope variations, including the Lomagundi positive carbon isotope excursion constrained to occur between 2306–2221 and 2106–2057 Ma (e.g. Bekker et al., 2006; Martin et al., 2013). It is the earliest, longest, and largest positive carbon isotope excursion known in marine carbonates that records a fundamental change in the global carbon cycle and oxygenation of the atmosphere–ocean system (Karhu and Holland, 1996; Bekker and Holland, 2012; Bekker, 2022). The Lomagundi carbon isotope excursion (LCIE) has now been found on all continents except Antarctica in unmetamorphosed sedimentary to granulite-facies metamorphic successions (Baker and Fallick, 1989a; Baker and Fallick, 1989b; Master et al., 2013; Bekker, 2022; Li et al., 2022).

The Fennoscandian Shield experienced protracted, multi-stage extension in the early Paleoproterozoic (2.5–1.95 Ga) that led to deposition of volcano-sedimentary successions and culminated with the breakup of the Archean craton (e.g. Lahtinen et al., 2008; Lahtinen and Köykkä, 2020). However, the associated rift stratigraphy and chemostratigraphic evolution of the northern part of the Fennoscandian Shield are still poorly understood and are not calibrated with high-precision age constraints. For example, the Karasjok Greenstone Belt (KGB; see Fig. 1) represents one of the major volcano-sedimentary rift structures in northern Fennoscandia, but lacks critical geochronologic and chemostratigraphic data.

Regional stratigraphic subdivisions for the KGB have been established (Siedlecka et al., 1985; Davidsen, 1994; Nilsen, 1998; Roberts and Davidsen, 2011; Siedlecka et al., 2011), but very little geochronological data have been published since the mid-1980s (i.e. Krill et al., 1985). Therefore, direct and precise geochronology for the northern part of the Fennoscandian Shield is still needed to unravel the volcano-sedimentary history, chemostratigraphy, and tectonic evolution of the region, and to better understand how it fits into a global context.

The goal of this study is to present and discuss new geochronologic and chemostratigraphic data for the rift-related units in the northern part of the KGB, and to compare them with other Paleoproterozoic units on the Fennoscandian Shield with respect to their tectonic settings, magmatic processes, and depositional reconstructions. The U-Pb zircon data set is combined with $\delta^{13}C$ isotope composition of the early Paleoproterozoic carbonate rocks, enabling a link to the global, Paleoproterozoic Lomagundi carbon isotope excursion.

2. Geological background

The Karasjok Greenstone Belt (KGB) is located in the northwestern part of the Fennoscandian Shield and consists of 2.5–1.95 Ga rift-related volcano-sedimentary and intrusive rocks (Siedlecka, 1985; Siedlecka et al., 1985; Braathen and Davidsen, 2000). The belt is c. 160 km long and 40 km wide on the Norwegian side of the border with Finland, and continues as the Central Lapland Greenstone Belt southward through Finland and Russia (see Fig. 1 and text below; Lahtinen et al., 2008; Lahtinen and Köykkä, 2020).

2.1. Tectonic evolution of the Fennoscandian Shield

The Archean and Paleoproterozoic history of the Fennoscandian Shield is well established through numerous studies (e.g., Gaál and Gorbatschev, 1987; Lahtinen et al., 2008; Melezhik and Hanski, 2013b). The oldest events led to the assembly of an Archean nucleus composed of the joined Kola and Karelia cratons (c. 2.9 Ga) (Fig. 1B), which were incorporated into the Late Archean Superia supercraton (see Bleeker, 2003). This was followed by protracted, multi-stage continental rifting and ultimate breakup in the early Paleoproterozoic (c. 2.5–1.95 Ga; e.g., Lahtinen et al., 2008; Lahtinen and Köykkä, 2020). Below, we briefly describe these rifting events and the breakup as a framework for the present study of the KGB.

Initiation of deposition of the c. 2505–2430 Ma *Sumian system*[1] on the Fennoscandian Shield (Hanski and Melezhik, 2013) was related to a magmatic plume below the Karelian and Kola cratons initiating rifting and the emplacement of a Large Igneous Province (LIP) that extensively covered the continent (Hanski, 2013). Rifting of the Superia supercraton started at the beginning of the Paleoproterozoic (Heaman, 1997; Ernst and Bleeker, 2010; Ciborowski et al., 2015) and involved several failed attempts. The earliest rifting episode on the Fennoscandian Shield is recorded on the Kola and northern Karelia cratons, where a NW–SE-elongated system (all directions refer to present-day geography) of layered intrusions was emplaced at c. 2.53–2.44 Ga (Amelin et al., 1995; Bayanova et al., 2009; Bayanova et al., 2019). Associated volcanic units developed on Archean basement are preserved in rift basins. These basins include the Imandra-Varzuga, Pechenga, Salla, Paanajärvi, Shambozero/Lekhta, and Vetreny greenstone belts in Russia and Finland that were deposited at c. 2.45–2.43 Ga (Sharkov and Smolkin, 1997; Chashchin et al., 2008; Vrevsky, 2011; Hanski and Melezhik, 2013) and contain thick intervals of rhyolitic, andesitic, and komatiitic volcanics. Comagmatic mafic to ultramafic layered intrusions, sills and dike complexes derived from the same komatiitic parental magmas were emplaced into the supracrustal sequences and the surrounding Archean basement (Puchtel et al., 1997; Puchtel et al., 2001; Kulikov et al., 2008; Kulikov et al., 2010; Myskova et al., 2013).

Large volumes of magma intruded the central part of the Karelia craton at c. 2.44 Ga (Mutanen and Huhma, 2001; Perttunen and Vaasjoki, 2001; Huhma et al., 2018). Plume-derived mafic magmas formed layered intrusions of the Tornio–Näränkävaara intrusive belt in Finland (Iljina and Hanski, 2005; Iljina et al., 2015; Yang et al., 2016; Maier et al., 2018; Järvinen et al., 2019). A-type granites, spatially associated with the mafic-to-ultramafic layered intrusions, were emplaced at the same time (Lauri and Mänttäri, 2002; Lauri et al., 2012). Comagmatic and geographically extensive dike swarms are also associated with continental rifting in the early Paleoproterozoic and show spatial and temporal relationships with the layered intrusions (Vuollo and Huhma, 2005; Stepanova et al., 2015). The volcanogenic Salla Group, which is the lowest unit of the Central Lapland Greenstone Belt in Finland, was deposited prior to the emplacement of the c. 2.44 Ga layered intrusions (Hanski and Huhma, 2005; Huhma et al., 2018; Köykkä et al., 2019).

After the Sumian group was deposited, Fennoscandia underwent deep weathering and erosion, which partially exposed the layered intrusions. The topography at that time is assumed to have been differentiated with deeply incised rift valleys and uplifted rift shoulders (Ojakangas et al., 2001; Melezhik and Hanski, 2013b).

[1] Sumian, Sariolian, Jatulian, and Ludicovian systems are informal stratigraphic subdivisions on the Fennoscandian Shield, equivalent to the regional stratigraphic horizons that extend across the whole shield and transcend individual sedimentary basins.

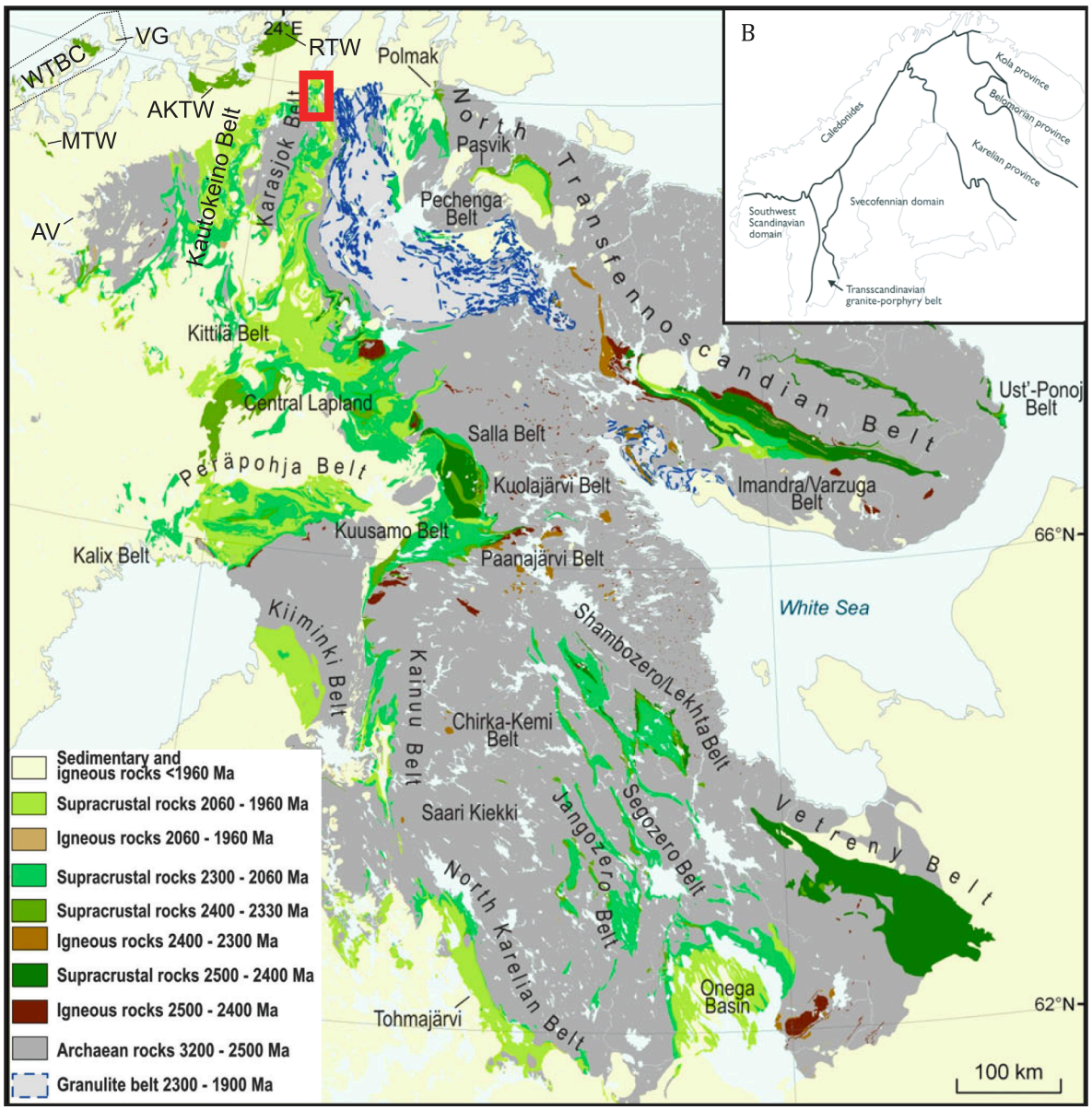

Fig. 1. A) Geological map of the northern Fennoscandian Shield. Red box indicates the study area (see Fig. 2). Abbreviations: WTBC = West Troms Basement Complex, VG = Vanna Group, AKTW = Alta-kVænangen Tectonic Window, RTW = Repparfjord Tectonic Window, MTW = Mauken Tectonic Window, AV = Altevatnet (modified from Melezhik and Hanski, 2013a). **B)** Major tectonic units of the Fennoscandian Shield (from Lahtinen et al., 2005).

The rocks of the c. 2.43–2.30 Ga *Sariolian system* were deposited on the Sumian–Sariolian unconformity, which is developed over large areas of the Fennoscandian Shield (Ojakangas et al., 2001). In general, age constraints for the Sariolian system are poor. It lies unconformably on the 2.44 Ga layered intrusions and is cut by rarely developed c. 2.32 Ga and widespread c. 2.22 Ga dikes (Vuollo and Huhma, 2005). Most *Sariolian* volcanic rocks are subaerial basaltic komatiites to basaltic andesites that show a strong crustal signature (Hanski, 2013). A prominent feature of the *Sariolian* clastic sedimentary rocks on the Karelian craton is the presence of diamictites and dropstones, interpreted as glacial deposits related to the Huronian-age global glaciations (Ojakangas et al., 2001; Melezhik et al., 2013). The top of the *Sariolian* system is, in several places, marked by an up to 20 m-thick paleoweathering crust (Ojakangas et al., 2001).

The c. 2.3–2.06 Ga *Jatulian* system sits on the unconformity and locally developed paleosoils and contains carbonate rocks that record the Lomagundi positive carbon isotope excursion (Karhu, 1993; Hanski and Melezhik, 2013). These rocks are widespread on the Fennoscandian Shield and were deposited both directly on the Archean basement and on older supracrustal successions and show a large variation in lithology from terrestrial siliciclastic and mafic volcanic deposits in the lower part to marine sedimentary and exhalative rocks in the upper part (Skuf'in and Theart, 2005; Hanski and Melezhik, 2013; Alfimova et al., 2022).

Jatulian magmatism is dominated by mafic volcanic rocks with tholeiitic to alkaline composition, which erupted in a shallow-marine environment (Hanski, 2013). The oldest major magmatic event during this period occurred at around 2.22 Ga as a relatively short-lived pulse. In northern and eastern Finland, magmatic rocks are found as more than 100 km-long, differentiated sills that were emplaced into *Jatulian* quartzites and along the contact between Archean basement and Paleoproterozoic supracrustal sequences (Perttunen and Vaasjoki, 2001; Rastas et al., 2001; Vuollo and Huhma, 2005; Hanski et al., 2010; Hanski, 2013).

The largest magmatic event during the Jatulian occurred at c. 2.15–2.11 Ga. It marked a period of renewed crustal extension and rifting of the Fennoscandian Shield. Abundant Fe-rich tholeiitic dike

swarms and mafic and granitoid plutons were emplaced into the Archean basement and overlying supracrustal units on the Karelian craton (Perttunen and Vaasjoki, 2001; Rastas et al., 2001; Vuollo and Huhma, 2005; Stepanova and Stepanov, 2010). Ahtonen et al. (2007) related this felsic magmatism to magmatic underplating and melting of the lower Archean crust coeval with extension leading to thinning and crustal subsidence. At the same time, MORB-type tholeiitic basaltic magmatism produced dike swarms and volcanics associated with the early stages in the opening of the Kola and Svecofennian oceans (Skuf'in and Theart, 2005; Lahtinen et al., 2008; Stepanova et al., 2014).

The *Ludicovian* (2.06–1.96 Ga) system rests unconformably on the *Jatulian* succession. In general, the lower sedimentary part of this group is characterized by organic-rich shales and mudstones, carbonates, greywackes, and tholeiitic basalts, indicating deposition on a passive continental margin above the drowned carbonate platform in the aftermath of the LCIE (see Bekker and Eriksson, 2003). The upper part consists of a thick volcanic unit of tholeiitic basalts, komatiites and ferropicrites (Hanski and Melezhik, 2013). The associated *Ludicovian* magmatism can broadly be grouped in two major events. The earlier c. 2.06–2.05 Ga event produced layered intrusions, dikes, and primitive volcanic rocks (Mutanen and Huhma, 2001; Hanski et al., 2001; Hanski and Huhma, 2005; Perello et al., 2015; Orvik et al., 2022). The later c.

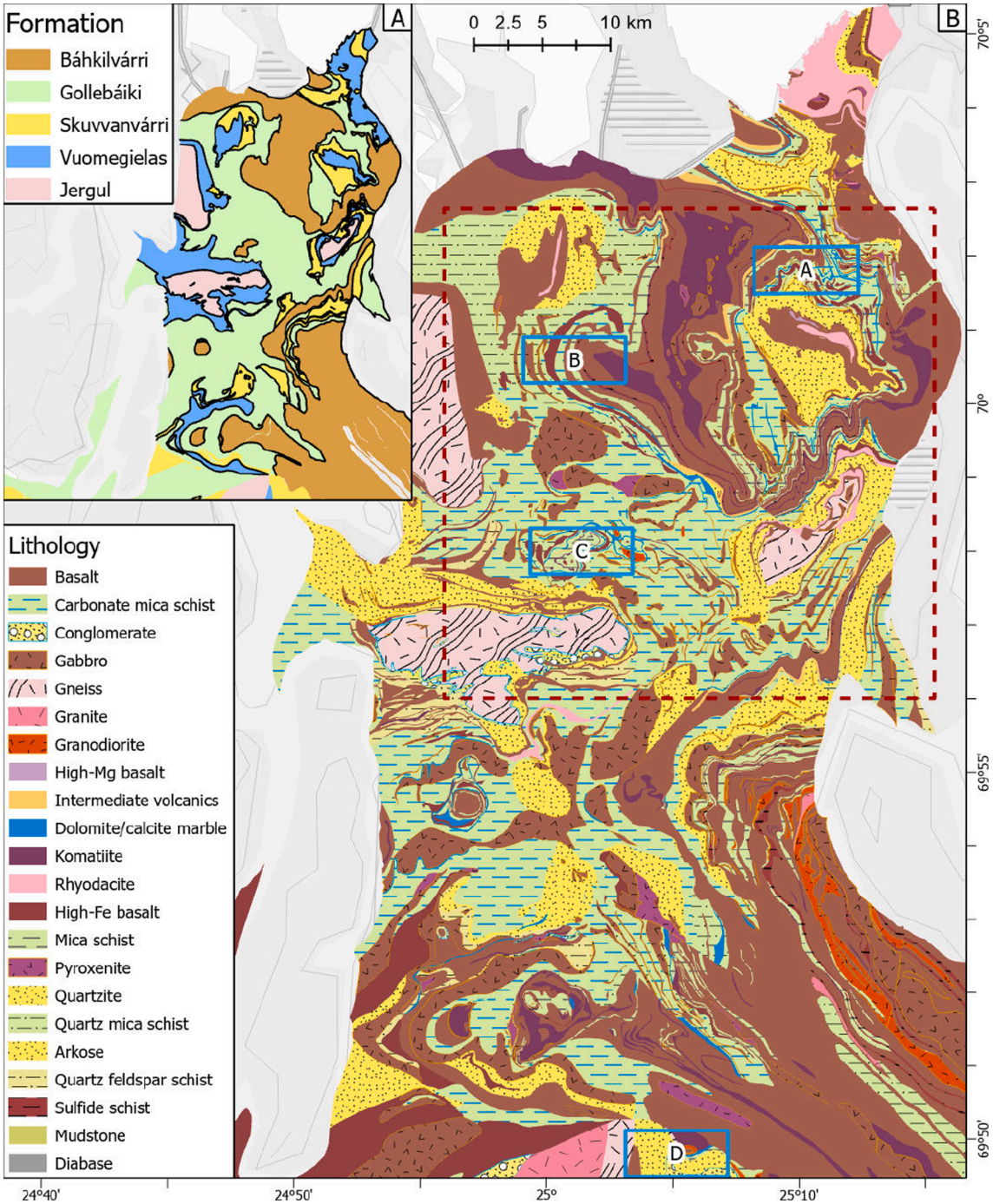

Fig. 2. A) Map of the northern part of the Karasjok Greenstone Belt, based on lithostratigraphy defined by Siedlecka et al. (1985). B) Bedrock map of the northern part of the Karasjok Greenstone Belt. Data compiled from Davidsen (1994); Nilsen (1998); Roberts and Davidsen (2011); Siedlecka et al. (2011). Blue boxes indicate carbonate sampling areas as seen in Fig. 4: A) Brittágielás, B) Porsvann, C) Lávvoaivi, D) Skuvvánvárri. Red dashed box indicates the extent of Fig. 6.

1.98–1.95 Ga event was dominated by flood basalts, picrites, and komatiites that are found both on the Kola and Karelian cratons (Puchtel et al., 1998; Puchtel et al., 1999).

The c. 500-million-year period of protracted, episodic rift-related magmatism and sedimentation ended with the Lapland-Kola orogeny at around 1.94 Ga when the Kola Ocean closed. This orogeny led to a Himalayan-scale mountain belt in the northern part of the Fenno-scandian Shield, the Lapland Granulite Belt, and basin inversion and deformation in the KGB (Daly et al., 2006).

2.2. The Karasjok Greenstone Belt

The KGB is sandwiched between the 2.98–2.78 Ga tonalite–-trondhjemite–granodiorite (TTG)-dominated Jergul gneiss complex (Bingen et al., 2015) in the west, and the Tanaelv Migmatite Belt to the east (Fig. 1). The latter consists of high- to medium-grade migmatites separated from the KGB by a west-verging ductile thrust (Krill, 1985; Braathen and Davidsen, 2000). Farther east, high-grade metasedimentary and mafic to intermediate igneous rocks of the Lapland Granulite Belt were thrusted on top of the Tanaelv Migmatite Belt (Krill, 1985; Gaál and Gorbatschev, 1987) during the c. 1.94–1.79 Ga Lapland-Kola and Svecofennian orogenic events (Lahtinen et al., 2008).

Previous tectonostratigraphic studies (Davidsen, 1994; Siedlecka et al., 1985; Braathen and Davidsen, 2000) showed that the northern KGB in the Lakselv area is dominated by a ~1500 m-thick succession of low- to medium-grade clastic sedimentary and volcanic rocks deposited in a rift to passive margin setting (Figs. 2 and 3), during the Sumian to Ludicovian time interval (c. 2.5–1.95 Ga). The Lakselv area also contains widespread mafic intrusions emplaced into the middle and upper parts of the stratigraphy (Fig. 3). There is no evidence of major tectonic breaks or shear zones that could have repeated units in the study area, although the presence of such structures cannot be discounted (Stokmo, 2020). The Lakselv area is therefore well suited for detailed geochronologic and chemostratigraphic studies (see Davidsen, 1994; Braathen and Davidsen, 2000; Stokmo, 2020). We thus consider the approximately 1500 m-thick rock package as a lithostratigraphic sequence. In this paper, the stratigraphy and formation names defined by Siedlecka et al. (1985) are used as outlined below.

2.2.1. Jergul Gneiss Complex

The Jergul Gneiss Complex is the oldest unit found in the region, previously dated at c. 2.98–2.78 Ga by Bingen et al. (2015). It is present in three separate tectonic windows in the northern part of the KGB. The complex in the Lakselv area is dominated by gray, compositionally layered, tonalitic, and partly mylonitic gneisses. Intrusive rocks such as granite, granodiorite, and mafic to ultramafic intrusions are also found farther south in the complex (Olesen and Sandstad, 1993).

2.2.2. The Vuomegielas Formation

The Vuomegielas Formation (previously called the Lavttevárri Formation by Braathen and Davidsen, 2000, , Fig. 3) is sparsely exposed in the KGB and consists mostly of homogenous foliated amphibolites interpreted to have a mafic volcanic precursor. It is the lowermost stratigraphic unit in the KGB and sits unconformably on the Jergul Gneiss Complex. The formation has experienced strong ductile deformation and is estimated by Davidsen (1994) to be at least 150 m thick. The lowest part of the formation consists of siliciclastic sedimentary rocks (Fig. 3). The basal contact is defined by conglomerates with clasts

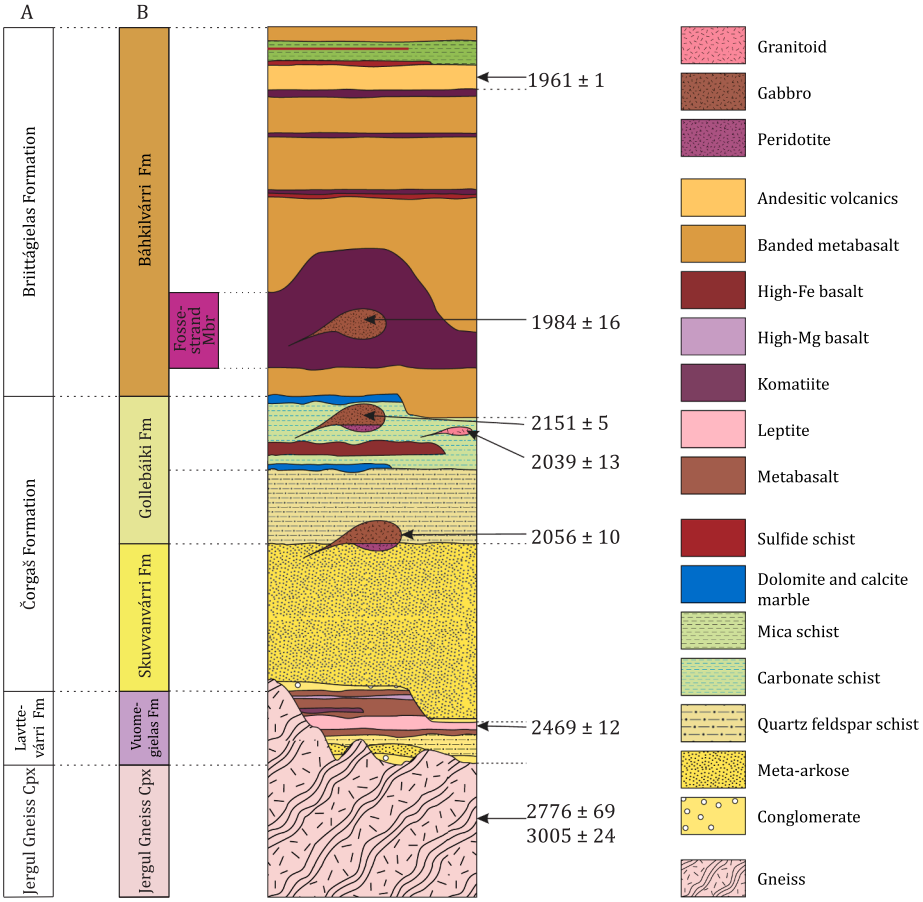

Fig. 3. Established lithostratigraphy with new U-Pb zircon data (this work) for the northern part of the Karasjok Greenstone Belt. Column A: Formation names used by Braathen and Davidsen (2000), column B: Formation names used in this study based on Siedlecka et al. (1985); Siedlecka et al. (2011); Roberts and Davidsen (2011). Ages are in million years (Ma) and uncertainties are given at the 2σ level.

of gneiss, quartz, and carbonates. The lower section also contains mica schist and quartzofeldspathic schist that is phyllosilicate- and carbonate-bearing. The upper part is dominated by volcanic rocks, mostly tholeiitic metabasalts and rhyodacites (the term 'leptite' has earlier been used by several authors); the latter was sampled for U-Pb geochronology in this study. Komatiites and high-Mg basalts are found interlayered with tholeiitic basalts (Davidsen, 1994; Siedlecka et al., 2011; Roberts and Davidsen, 2011).

2.2.3. The Skuvvanvárri Formation

The Skuvvanvárri Formation was estimated to be up to 1000 m thick and consists of terrigenous clastic sediments deposited unconformably on the Jergul Gneiss Complex and Vuomegielas Formation. Matrix-supported alluvial fan conglomerates and mature quartzites with minor amounts of pelites and carbonates dominate the formation. Clastic sedimentary rocks are commonly fuchsite-bearing, indicating ultramafic sources. Quartzites are well-sorted and, at some localities, show cross-bedding (Often, 1985; Siedlecka, 1985).). Gabbroic intrusions locally intrude the metasedimentary succession, one of which has been dated at c. 2.05 Ga (Orvik et al., 2022). This unit corresponds to the lower part of the Čorgaš Formation in the stratigraphy of Braathen and Davidsen (2000) (Fig. 3).

We have sampled and dated (U-Pb zircon) the Porsvann intrusion (Fig. 7C), a prominent body of Ni-Cu-PGE-mineralized metapyroxenites and metagabbros that intruded the quartzofeldspathic schists of the Skuvvanvárri Formation (Nilsson and Often, 2005).

2.2.4. The Gollebáiki Formation

The Gollebáiki Formation is c. 1000–1500 m thick and characterized by laterally variable volcanogenic and sedimentary facies. The lower part of the formation contains mafic to komatiitic volcanic rocks with exhalative chert horizons. The middle part is dominated by carbonates and quartzofeldspathic mica schists (Fig. 2.2), and the upper part of the formation comprises psammites and minor amounts of tholeiitic volcanic rocks, locally cut by quartz-dioritic dikes. The volcanic units are interlayered with thin carbonate and pelite beds. The psammite is albite-bearing; elevated concentrations of sodium suggest the presence of evaporites in the sedimentary precursors (see Melezhik et al., 2015). Sedimentary structures indicate a near-shore to tidal-marine depositional environment. The upper part comprises marble and mica-schist (Often, 1985; Siedlecka et al., 1985; Elvebakk et al., 1985). In the northern KGB, this formation corresponds to the upper part of the Čorgaš Formation, as defined by Braathen and Davidsen (2000) (Fig. 3). We sampled the northern part of the Čoalbmejávri intrusion (Hansen, 2008), located in the middle of the formation (Hansen, 2008), for U-Pb zircon dating.

2.2.5. The Báhkilvárri Formation

The Báhkilvárri Formation is 300 to 700 m thick and sits with an angular and erosional unconformity on the Gollebáiki Formation. It contains compositionally layered, garnet-bearing amphibolites interpreted to represent tholeiitic basaltic lavas. The Fossestrand Member is in the lower part of the formation (Fig. 2.2) and and is a c. 250 m-thick unit consisting of well-preserved komatiites and coeval gabbroic intrusions. Primary structures, such as pillow lavas and pyroclastic deposits, indicate deposition in a shallow, subaqueous setting (Barnes and Often, 1990; Davidsen, 1994). Krill et al. (1985) obtained a whole-rock Sm-Nd isochron date of 2085 ± 85 Ma for the komatiites in the KGB. Banded iron formations and sulfide-bearing exhalites are associated with the komatiites (Often, 1985). A section of pelites and intermediate volcanic rocks overlies the basalts. The upper part of the formation is a section of 50–70 m-thick pelites and andesitic volcanics.

2.3. Deformation and structural architecture of the KGB

The KGB underwent multiple episodes of ductile compressional deformation during the 1.94–1.79 Ga Lapland-Kola and Svecofennian orogenies, when the 2.5–1.95 Ga rift basins and related Kola Ocean closed, associated with and followed by arc magmatism, accretion, and continent–continent collision between the Kola and Karelian cratons (Daly et al., 2006; Lahtinen et al., 2005; Lahtinen et al., 2008). In the KGB these orogenic events involved (see Fig. 2) E–W compression with regional-scale folding and thrusting (D_1 event), producing a pervasive foliation subparallel to lithological contacts, followed by low-angle thrusting along west-dipping mylonite zones (Krill, 1985; Braathen and Davidsen, 2000; Stokmo, 2020). These structures formed under amphibolite-facies conditions (Davidsen, 1994; Braathen and Davidsen, 2000).

Later, NE–SW-directed shortening (D_2 event) produced SW-verging shear folds (F_2) and related ductile thrusts at the base of ultramafic intrusions. Mineral assemblages indicate retrograde greenschist-facies alteration (Braathen, 1993; Andreassen, 1993; Davidsen, 1994; Braathen and Davidsen, 2000).

The youngest superimposed structures (D_3 event) include map-scale, steeply N- and S-plunging chevron folds (F_3) and minor ductile shear zones along modified fold limbs, still at greenschist-facies conditions (Braathen and Davidsen, 2000; Stokmo, 2020).

2.4. Geology of coeval Paleoproterozoic greenstone belts in the northern Fennoscandian Shield

Volcano-sedimentary and magmatic units in the northern Fennoscandian Shield coeval with the KGB are described below.

2.4.1. Repparfjord Tectonic Window

The Repparfjord Tectonic Window is exposed in the northern part of the Scandinavian Caledonides (Fig. 1) and and consists of a ~8 km-thick volcano-sedimentary succession divided into four distinct groups (Pharaoh et al., 1983): The *Saltvatnet Group* is the lowermost unit and consists of coarse-grained fluvial sandstones and conglomerates, deposited on alluvial fans, along with siltstone and slate with interlayered dolostone representing submarine debris flows. The dominant lithologies in the overlying *Holmvatnet Group* are basaltic to andesitic lava and tuff with interlayered volcanoclastic sandstones. The overlying *Nussir Group* also contains basaltic lava flows, pillow lavas, and tuffs. The uppermost *Porsa Group* contains shallow-marine sedimentary rocks such as dolostone, graphitic shale and intercalated sandstone, tuff, and stromatolitic carbonates (Pharaoh et al., 1983; Torgersen et al., 2015). LA-ICP-MS U-Pb zircon dating carried out by Perello et al. (2015) on a tuffaceous horizon in the Nussir Group gave an age of 2073 $^{+23}_{-12}$ Ma.

2.4.2. Alta-kVænangen Tectonic Window

The Alta-kVænangen Tectonic Window covers an area southwest of the Repparfjord Tectonic Window (Fig. 1) and is considered to be a continuation of the Kautokeino Greenstone Belt, based on regional geophysics (Olesen and Sandstad, 1993; Nasuti et al., 2015). ZZwaan and Gauthierwaan and Gauthier (1980) divided the Alta-kVænangen Tectonic Window into four formations. The lowermost *Kvenvik Formation* consists of a >1500 m-thick sequence of predominantly tholeiitic metabasalts, layers of dolostone, and synvolcanic gabbroic intrusions (Bergh and Torske, 1988). The overlying ~600 m-thick *Storviknes Formation* consists of dolostone and shale deposited in a shallow-marine environment (ZZwaan and Gauthierwaan and Gauthier, 1980; Melezhik et al., 2015). The superimposed *Skoađđovárri Formation* is more than 1700 m thick and contains mainly sandstones with conglomerates and shale layers. It has been interpreted to be fluviomarine/deltaic, with alluvial sediments (Bergh and Torske, 1986). The uppermost *Luovosvárri Formation* consists of stromatolitic dolostones with sandstone (ZZwaan and Gauthierwaan and Gauthier, 1980).

U-Pb zircon geochronology of a synvolcanic gabbro in the Kvenvik Formation gave an age of 2146 ± 5 Ma (Melezhik et al., 2015). Carbon isotope values for dolostones of the same formation are highly positive

at + 7.4 ± 0.7 ‰ (n = 51; Melezhik et al., 2015). Carbonates from the overlying Storviknes Formation have $\delta^{13}C$ values of + 1.1 ± 1.2 ‰ (n = 41), indicating that the latter unit was deposited after the end of the LCIE and therefore younger than c. 2060 Ma (Melezhik et al., 2015).

2.4.3. Kautokeino Greenstone Belt

The Kautokeino Greenstone Belt is located in western Finnmark and is a ~40–60 km-wide and 120 km-long NNW-SSE-trending supracrustal belt separated from the KGB by the Jergul Gneiss Complex (Fig. 1, Henderson et al., 2015).

The Archean *Goldenvárri Formation* is the lowermost unit of the Kautokeino Greenstone Belt and is 1–1.5 km thick (Solli, 1983), mainly composed of tholeiitic metabasalts and is spatially associated with the Jergul Gneiss Complex. U-Pb dating of zircon from a trachyandesite layer by Bingen et al. (2015) gave an age of 2781 ± 4 Ma.

The 500–1000 m-thick *Masi Formation* is dominated by fine-grained, fuchsite-rich quartzite interlayered with conglomerates. It lies unconformably on the Goldenvárri Formation and the Jergul Gneiss Complex and the contact is typically marked by a ~5 m-thick basal conglomerate. The Masi Formation is correlated, based on stratigraphy and lithology, with the Skuvvanvárri Formation in the KGB (Siedlecka, 1985; Solli, 1983). Bingen et al. (2015) dated with the U-Pb zircon method a diabase sill within the Masi Formation at 2220 ± 7 Ma, providing a minimum age for the formation.

The *Suoluvuopmi Formation* conformably overlies the Masi Formation and consists of mica schist, graphite schist, metabasalt and some minor metakomatiite (Solli, 1983; Siedlecka et al., 1985). So far, there has not been any successful attempt at directly dating the lithologies of this formation. The formation is cut by geochemically similar dikes as the one dated in the Masi Formation, which suggests that its depositional age might be older than 2220 ± 7 Ma (Bingen et al., 2015).

The 7–8 km-thick *Lik'ča Formation* is developed in the eastern part of the Kautokeino Greenstone Belt. It contains tholeiitic metabasalts with primary structures such as pillows and tuffs, and interlayered with graphitic schist, sandstone, and dolostone (Siedlecka et al., 1985). A tonalitic pluton that intruded the formation yielded an age of 1955 ± 7 Ma (Bingen et al., 2015). The *Čas'kejas Formation* in the western part of the Kautokeino Greenstone Belt is correlative with the Lik'ča Formation. It consists of a ~4 km-thick sequence of layered and massive subalkaline metavolcanic rocks interbedded with subordinate layers of carbonate, "albite felsite", and graphitic schist. The upper part of the formation contains mica schist and phyllite with graphitic schist and dolostone layers (Siedlecka et al., 1985). A synvolcanic gabbro has been dated at 2147 ± 5 Ma, which provides the age for the Čas'kejas Formation magmatism (Bingen et al., 2015).

The *Bihkkačohka Formation* overlies the Čas'kejas Formation with a transitional stratigraphical contact. The lower part of the formation is dominated by feldspathic sandstone, while the upper part is composed of shale and siltstone. The uppermost formation in the Kautokeino Greenstone Belt is the *Čáravárri Formation*, a coarse-grained sandstone interlayered with alluvial conglomerates. No geochronological data are available for these two uppermost formations, but the Čáravárri Formation has earlier been correlated with the Skoađđovárri Formation in the Alta-kVænangen Tectonic Window (Torske and Bergh, 2004), suggesting that it is younger than c. 2060 Ma.

2.4.4. Central Lapland Greenstone Belt

The Central Lapland Greenstone Belt is the continuation of the Karasjok Greenstone Belt into northern Finland (Fig. 1) (Fig. 1; Hanski and Huhma, 2005). It has, until now, been difficult to correlate the stratigraphy across the border due to a lack of precise age determinations on the Norwegian side.

The *Salla Group* is the lowermost Paleoproterozoic unit in the Central Lapland Greenstone Belt. It mostly occurs in the southern part of the belt and is dominated by 2426 ± 6 and 2438 ± 11 Ma felsic and intermediate volcanic rocks erupted under subaerial conditions (Räsänen and Huhma, 2001; Manninen et al., 2001; Hanski and Huhma, 2005) and intruded by the 2439 ± 3 Ma Koitelainen and 2436 ± 6 Ma Akanvaara mafic, layered intrusions (Mutanen and Huhma, 2001; Huhma et al., 2018). The age of the overlying *Kuusamo Group* sits on top of several meter-thick Al-rich paleosols at the top of the Salla Group and starts with a 10 meter-thick conglomerate and sericitic schist. It consists of tholeiitic and komatiitic volcanic rocks that have been deposited in a predominantly subaerial environment (Hanski and Huhma, 2005). The depositional age of the Kuusamo Group is bracketed between the age of the underlying Salla Group (c. 2.43–2.44 Ga) and a 2403 ± 3 Ma cross-cutting mafic dike (Huhma et al., 2018).

Thick units of quartzite and mica schist dominate the *Sodankylä Group* with interlayered sequences of carbonates and evaporites. They were deposited on the underlying volcanic lithologies or directly on the Archean basement. The sedimentary environment was a tidally influenced, shallow-marine setting. The age of the group is between c 2.35–2.33 Ga (age of youngest detrital zircons; Köykkä et al., 2019) and a 2213 ± 14 Ma (zircon Pb-Pb age of intruding mafic sills; Huhma et al., 2018). The carbonates of the Sodankylä Group record the rising trend in carbon isotope values up to >10 ‰, corresponding to the peak of the Lomagundi carbon isotope excursion Karhu, 1993. The Salla, Kuusamo, and Sodankylä groups were deposited in a rift setting during protracted, multi-stage continental extension in the early Paleoproterozoic.

The *Savukoski Group* consists of a lower part of black schist, greywacke, thin carbonates, and an upper volcanogenic part dominated by ultramafic and mafic units; it was deposited on a passive continental margin (Köykkä et al., 2019). The 2148 ± 11 Ma Rantavaara gabbro and 2058 ± 5 Ma Kevitsa intrusion and several cross-cutting diabase dikes provide a minimum depositional age for the group (Mutanen and Huhma, 2001; Huhma et al., 2018). The carbonates of the Savukoski Group record the falling trend in carbon isotope values down to ~0 ‰, corresponding to the end of the Lomagundi carbon isotope excursion (Karhu, 1993).

The *Kumpu Group* is the uppermost group in the Central Lapland Greenstone Belt and was deposited in the foreland basin (Köykkä et al., 2019). It is mainly composed of quartzite with intervals of conglomerate and felsic volcanic rocks. The maximum depositional age is constrained by 1.88 Ga granitic pebbles in the conglomerate (Huhma et al., 2018).

3. Carbonate sampling

We sampled carbonates throughout the stratigraphy of the KGB in order to determine the carbon and oxygen isotope compositions (Table 2). Sampling sites include four locations: Brittágielas, Porsvann, Lávvoaivi and Skuvvanvárri, and represent the three uppermost formations in the KGB, i.e., Skuvanvarri, Gollebáiki, and Báhkilvárri formations (Fig. 4 and Table 2).

The stratigraphically lowermost carbonates are from the Skuvanvarri Formation, taken at three different localities in its type area (Fig. 4D). Two samples are from weathered, micaceous carbonate layers within a mica schist sequence (*KGB-05* and *KGB-06*). The stratigraphically lowest sample (*KGB-07*) is from the upper part of the basal conglomerate. It consists of angular clasts of carbonates and siliciclastic material in a fuchsite- and carbonate-bearing matrix (Fig. 5A).

We collected two samples from the lower Gollebáiki Formation in the Brittágielás area; one from the same carbonate unit (Fig. 5B; Table 2; sample *KGB-01*) that was extensively sampled by Melezhik et al. (2015) and one sample from a mica schist unit (*KGB-08*). Three different localities of the formation were sampled in the Porsvann area (Fig. 4B): a ~1 m-thick carbonate layer located next to the Porsvann intrusion (*KGB-02*), and a 1–2 m-thick, copper-bearing Fe-rich carbonate lens within a metavolcanic unit (*KGB-03*). The sample contains up to 10 mm clusters of bornite and pseudomorphs of evaporite minerals (Fig. 5c). The last sample is from a large~10 m-high cliff of red to pink dolomitic marble in the eastern part of the area (*KGB-04*).

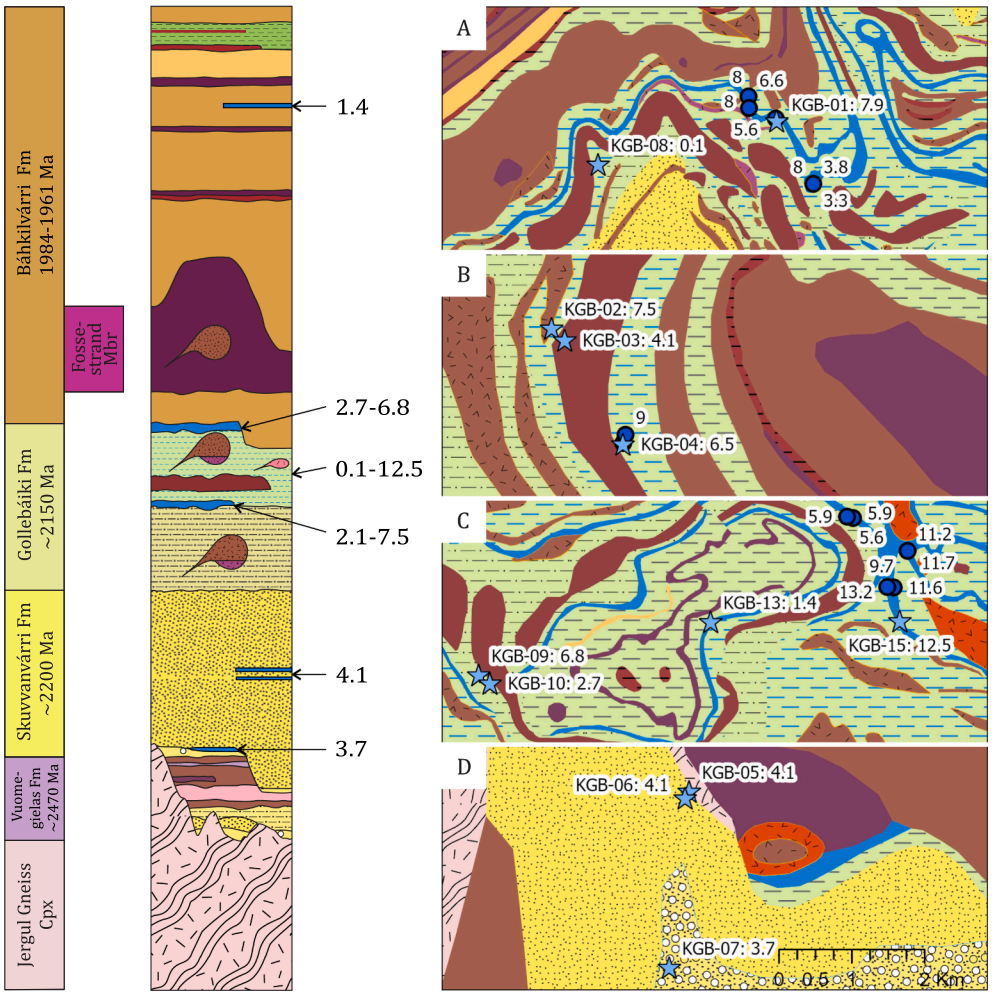

Fig. 4. Schematic stratigraphy and location maps for sampled carbonates in the KGB. All values are $\delta^{13}C$ ‰, VPDB. Samples marked with stars are from this study (Table 2), circles are from Melezhik et al. (2015). Map areas as marked in Fig. 2: **A)** The Brittágielas area, samples taken from the Gollebáiki Formation. **B)** Porsvann, carbonate samples taken from Gollebáiki Formation **C)** Lávvoaivi, samples taken from the Gollebáiki and Báhkilvárre formations. **D)** Skuvvánvárri, samples taken from the basal and middel part of the Skuvvánvarri Formation.

In the Lávvoaivi area we sampled the two uppermost formations of the KGB, i.e., three samples from the Gollebáiki Formation and one from the Báhkilvárre Formation (Fig. 4C, Table 2). Samples *KGB-09* and *KGB-10* are both from ~1 m-thick carbonate layers within the Gollebáiki Formation metavolcanic rocks. Notably, these carbonates also contain pseudomorphs of evaporite minerals. Sample *KGB-15* is from the eastern part of the area and it is taken from a 2 m-thick carbonate unit above a 3–5 m-thick collapse breccia of carbonates hosted by a mica schist unit. All of these samples are from the Gollebáiki Formation. The fourth sample (*KGB-13*) is from the uppermost stratigraphic level found in the area, interpreted to be the Báhkilvárre Formation.

4. Sample descriptions and U-Pb geochronology results

First, we present new geochronological data for the Jergul Gneiss Complex and volcanic formations and intrusive rocks from the overlying KGB (Table 1), utilizing the established stratigraphy for the KGB (see Section 2.2). After that, we will describe the chemostratigraphic results ($\delta^{13}C$ and $\delta^{18}O$) for carbonates from stratigraphically different positions in the KGB (Table 2). See electronic supplement for methods and analytical work.

As discussed below, the zircon grains analyzed in this study are texturally complex and appear variably altered. The geochronological data for most samples reflect this textural complexity and display evidence of Pb loss (mainly Caledonian) and incorporation of common Pb. In an attempt to alleviate some of the inherent subjectivity in interpreting such data, we have calculated the percentage of common Pb for each analysis for samples where this appears to be an issue, typically reflected in analyses plotting well above discordias in Tera-Wasserburg plots. Along with statistical identification of outliers, this is the main tool for deciding which analyses to include in regressions. The percentage of common Pb was calculated by assuming that the 204 signal measured on GJ, the primary standard is from ^{204}Hg, i.e., no ^{204}Pb, as suggested by TIMS analyses (Jackson et al., 2004). Plots were made and ages calculated using Isoplot (Ludwig, 2008).

4.1. Jergul Gneiss Complex

The Jergul Gneiss Complex constitutes the basement of the Karasjok Greenstone Belt. It can be found in several tectonic windows inside the KGB (Fig. 2 and 6), in addition to the area between the Karasjok and Kautokeino greenstone belts. The unit consists of several different lithologies, but tonalitic gneiss is the most common. Granitic, granodioritic, and mafic units are also found. We have collected two samples from a tectonic window north of Skoganvarre (Fig. 6 and Table 1).

Sample *2018-HAH-103* is a gray, compositionally layered and partly migmatized tonalitic gneiss (Fig. 7A). The rock consists of quartz, strongly sericitized plagioclase porphyroblasts, biotite, and chlorite (see Figs. 6, 8A, and 8B). The zircon grains are euhedral to subhedral prismatic, indicating a magmatic origin. Their size is ~100–150 μm along the c-axis. The zircons have a partly anhedral core showing oscillatory zoning and a euhedral homogenous rim (see electronic supplement B for images). We carried out 24 analyses on this sample, both on zircon rims and cores. Most of the analyses cluster around 3000 Ma and define a discordia with upper and lower intercepts of 3005 ± 24 and 1389 ± 230 Ma, respectively (MSWD = 2.7, Fig. 9A). The former is considered to

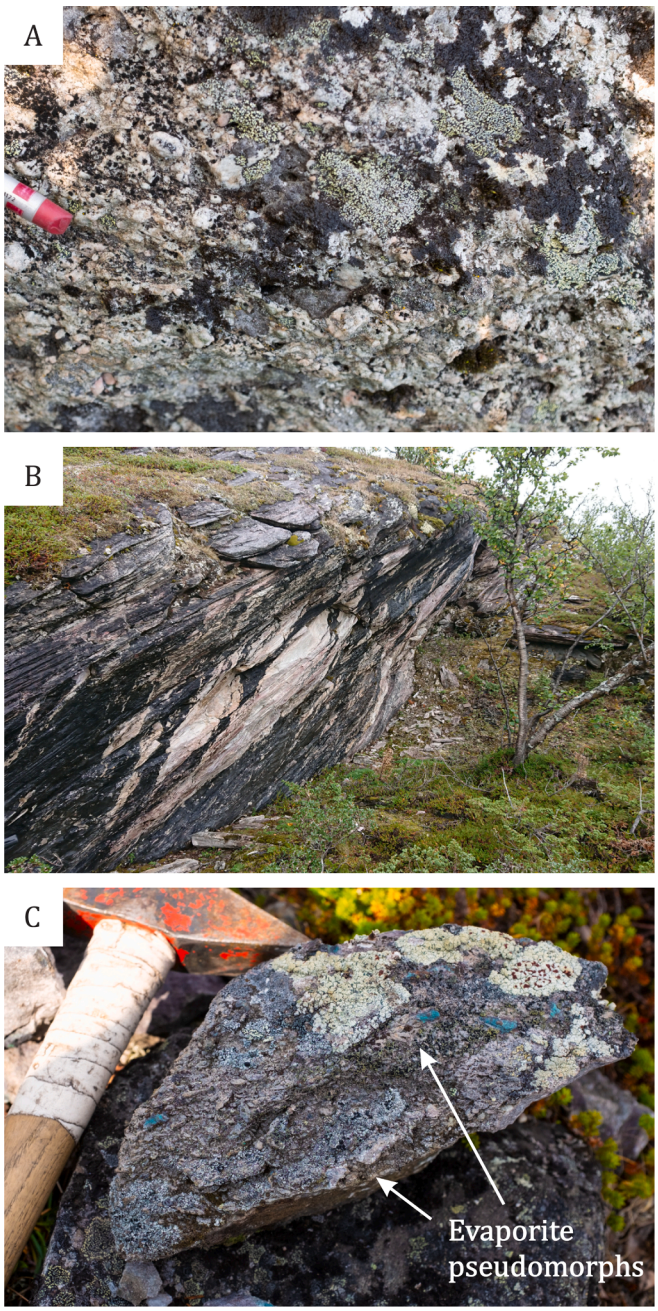

Fig. 5. Outcrops showing selected carbonates sampled for isotope analysis. **A)** Fuchsite-bearing conglomerate (gritstone) from the Skuvvánvárri area with calcatreous matrix and clasts. The sample is taken from the upper part of the basal conglomerate of the Skuvvánvárri Formation (*KGB-07*). **B)** Dolomite marble from the Brittágielas area (sample *KGB-01*). The outcrop is c. 1.5 m high. **C)** Bornite-bearing carbonate from the Porsvann area taken from a 1–2 m-thick Fe-rich carbonate layer in metabasalts of the Gollebáiki Formation. Note the presence of evaporite pseudomorphs (sample *KGB-03*).

reflect the crystallization age of the protolith to the tonalitic gneiss, whereas the significance of the imprecise lower intercept, if any, is unknown. The U-Pb data show no systematic age difference between zircon cores and rims, and the geologic significance of the rims is unknown.

2018-HAH-105 is a tonalitic, hematite-stained gneiss taken from the same tectonic window in Skoganvárre, 445 m southeast of sample 2018-HAH-103. The zircon grains are 75–100 μm long and sub-rounded in shape. Most of the 35 measured zircon grains show no or weak oscillatory zoning in CL, are discordant and do not form any well-defined discordia line (Fig. 9B). A regression through all analyses yields upper and lower intercept dates of 2776 ± 69 and 277 ± 63 Ma (MSWD = 40), respectively. The most discordant analyses are generally high in common Pb, suggesting that the zircon grains were open to post-crystallization diffusion. However, excluding analyses with high common Pb does not result in a regression with better fit. The oldest concordant grain has a date of 2818 ± 15 Ma and the youngest a date of 2599 ± 15 Ma (Fig. 9B). The data can be interpreted in different ways. A likely interpretation is that the sample is a paragneiss and the dated zircons are detrital. It is also possible that the protolith is c. 2.8 Ga old, overprinted by the late Archean metamorphic event seen elsewhere in NW Fennoscandia (e.g., Myhre et al., 2013; Slagstad et al., 2015). Alternatively, the protolith could be c. 2.6 Ga, with the older zircon grains representing inheritance. However, no magmatic activity of this age is known in the region, and we consider this interpretation to be the least likely.

4.2. *Vuomegielas Formation*

The only lithology of the Vuomegielas Formation from which we were able to separate zircons is a rhyodacite from the upper part of the stratigraphy (Figs. 3 and 7B). Zircons occur in this rock as inclusions in other minerals, which makes mineral separation difficult by gravity methods.

Sample *2018-HAH-100* (Fig. 6 and Table 1) contains poikilitic plagioclase in a matrix composed of fine-grained quartz, microcline, biotite, and amphibole. Accessory minerals include titanite, apatite, and pyrite, typically occurring as inclusions in plagioclase porphyroblasts (see Figs. 8C and 8D). The zircons are up to 250 μm in length and mostly represent broken fragments of larger zircons. Internally, the grains show chaotic and patchy textures in CL and have inclusions of, or are intergrown with titanite. Fourteen of 31 analyses are characterized by high common Pb, and a regression through the remaining 17 analyses yield upper and lower intercept ages of 2469 ± 12 and 391 ± 88 Ma, respectively (MSWD = 18, Fig. 9C). The former is interpreted to date crystallization of the rhyodacite and the latter most likely reflects Caledonian Pb loss.

4.3. *Skuvvanvárri Formation*

We were not able to identify any volcanic units in the Skuvanvárri Formation that would allow us to constrain the depositional age directly. Instead, we dated a sample from the Porsvann intrusion, the age of which provides a minimum depositional age for the formation.

4.3.1. *The Porsvann Intrusion*

Sample *2018-HAH-098* is from an anorthositic lens in the Cu/Ni-PGE mineralization at Porsvann (Fig. 7C). The hand specimen is rusty red in color and fine-grained. It consists of hematite-stained plagioclase, quartz, and amphibole. Minor phases are biotite, magnetite, ilmenite, and sulfides (Figs. 8G and H). The separated zircon grains are mostly fragments of larger, broken crystals. They are euhedral to subhedral, elongated prismatic crystals, up to c. 250 μm in length. CL images show that the zircons are variably chaotically and patchily zoned, but locally preserve oscillatory zoning. However, we do not see any systematic variation in age between different textural domains. Excluding 11 analyses with high common Pb, the remaining 24 analyses yield a poorly defined discordia with upper and lower intercept dates of 2082 ± 22 and 304 ± 24 Ma, respectively (MSWD = 57, Fig. 10A).Five analyses that are < 6% discordant yield a weighted average $^{207}Pb/^{206}Pb$ date of 2056 ± 10 Ma (MSWD = 3.4, Fig. 10B), considered to be the best estimate of the crystallization age of the anorthositic lens and the Porsvann intrusion. This age suggests that the Skuvvanvárri Formation was deposited prior to c. 2060 Ma.

Table 1
Summary of U-Pb zircon isotopic results for the northern part of the Karasjok Greenstone Belt. All ages are in million years (Ma).

Sample ID	Locality	Lat	Long	Unit[a]	Lithology	Petrography[b]	U-Pb age	±2σ	MSWD	n	Type
2018-HAH-103	Skoganvárre	69.942075	24.96495	Jergul Gneiss Cpx	Gneiss	Qtz, Plg, Bi	3005	24	2.7	24	Disc
2018-HAH-105	Skoganvárre	69.940926	24.96714	Jergul Gneiss Cpx	Gneiss	Qtz, Plg, Bi	2776	69	40	35	Disc[1]
2018-HAH-100	Porsvann	70.026039	25.00016	Vuomegielas Fm	Rhyodacite	Plg, Mic, Qtz	2469	12	18	17	Disc
2018-HAH-110	Coalbmejávri	69.98927	25.0261	Čoalbmejávri Int	Gabbro	Amp, Plg, Mt	2151	5	6.7	23	WA
2018-HAH-098	Porsvann	70.012339	24.99454	Porsvann Int	Anorthosite	Plg, Amp	2056	10	3.4	5	WA
2018-HAH-075	Brennelv	70.025885	25.14531	Gollebaiki Fm	Qtz-diorite	Plg, Qtz, Mt	2039	13	1.5	24	Disc
2018-HAH-029	Brennelv	70.034251	25.12063	Fossestrand Mbr	Gabbro	Amp, Plg	1984	16	39	11	WA
2019-HAH-112	Brennelv	70.033006	25.14306	Bahkilvárri Fm	Andesite	Plg, Amp, Bi	1961	2	10	20	WA
2018-HAH-021	Brennelv	70.035056	25.1511	Bahkilvárri Fm	Andesite	Plg, Amp, Bi	1962	11	0.7	22	Disc
2018-HAH-050	Brennelv	70.033002	25.14313	Bahkilvárri Fm	Andesite	Plg, Amp, Bi	1952	11	1	24	Disc

[c]Conc = Concordia age, WA = Weighted Average age.
[a] Cpx = Complex, Int = Intrusion, Fm = Formation
[b] Qtz = quartz, Plg = plagioclase, Mic = microcline, Bi = biotite, Amp = amphibole, Cpx = clinopyroxene, Mt = magnetite, S = Sulfides
[1] Sample is either a paragneiss or contains metamorphically altered zircons. Concordia grain ages spread from 2818 ± 15 Ma to 2599 ± 15 Ma

Table 2
Summary of C and O isotope values for carbonates from the Karasjok Greenstone Belt. Coordinates are given in decimal degrees, WGS 1984. See Section 3.2 for analytical uncertainties.

Sample ID	Long	Lat	Location	Mineralogy	$\delta^{13}C$[a]	$\delta^{18}O$[a]	%[b]
Báhkilvárre Formation:							
KGB-13	25.0225	69.9666	Lávvoaivi	Calcite	1.4	−15.8	97
Gollebáiki Formation:							
KGB-09	24.9939	69.9644	Lávvoaivi	Calcite	6.8	−14.4	65
KGB-10	24.9953	69.9640	Lávvoaivi	Calcite	2.7	−17.2	88
KGB-11	24.9953	69.9640	Lávvoaivi	Calcite	2.4	−16.7	55
KGB-12	24.9989	69.9642	Lávvoaivi	Dolomite	2.5	−22.6	5
KGB-15	25.0458	69.9667	Lávvoaivi	Dolomite	12.5	−13.1	96
KGB-01	25.1781	70.0304	Brittágielas	Dolomite	7.9	−13.2	90
KGB-08	25.1561	70.0286	Brittágielas	Calcite	0.1	−16.0	100
KGB-02	24.9984	70.0118	Porsvann	Calcite	2.1	−15.8	48
KGB-02–2	24.9984	70.0118	Porsvann	Calcite	7.5	−14.6	76
KGB-03	25.0000	70.0113	Porsvann	Dolomite	4.1	−19.0	56
KGB-04	25.0072	70.0069	Porsvann	Calcite	6.5	−13.4	62
Skuvvanvárri Formation:							
KGB-05	25.0826	69.8333	Skuvvanvárri	Dolomite	4.1	−20.6	32
KGB-06	25.0821	69.8330	Skuvvanvárri	Dolomite	4.1	−20.6	14
KGB-07	25.0802	69.8258	Skuvvanvárri	Dolomite	3.7	−21.8	10

[a] ‰, VPDB
[b] Approximate percentage of carbonate in sample

4.4. The Gollebáiki Formation

We were unable to identify zircon-bearing volcanic rocks in the Gollebáiki formation that would provide a direct depositional age of the formation. However, two intrusive units give ages that constrain the minimum depositional age of the formation.

4.4.1. The Čoalbmejávri Intrusion

The Čoalbmejávri layered intrusion outcrops in several mafic to ultramafic sections in the middle part of the study area (Fig. 2) where it intrudes into a sequence of carbonate-bearing, quartzofeldspathic schists of the Gollebáiki Formation. The intrusion is layered due to magmatic fractionation and contains lithologies ranging from peridotite to anorthosite (Hansen, 2008). Sample *2018-HAH-110* is a metagabbro (Fig. 7D), consisting of metamorphic amphibole replacing pyroxene, plagioclase, and remnants of partly metamorphosed augite and enstatite (Figs. 8E and F). Minor mineral phases are chlorite, titanite, magnetite, and iron sulfides. Extracted zircons are elongated, prismatic, and up to c. 300 μm along their longest axis. CL images show a variety of textures, from almost homogenous, to wavy, irregularly oscillatory, to chaotic, patchy zoning. Thirty of 31 analyses from this sample define a regression with upper and lower intercept dates of 2164 ± 23 and 587 ± 190 Ma, respectively (MSWD = 42, Fig. 9D). One analysis (#17) was excluded from the regression due to high common Pb. The majority of analyses are near concordant, with only three analyses > 10% discordant. The near-concordant analyses yield a weighted average $^{207}Pb/^{206}Pb$ age of 2151 ± 5 Ma (MSWD = 6.7, Fig. 9E, four analyses were recognized as statistical outliers by Isoplot and excluded). The age of 2151 ± 5 Ma is interpreted to date crystallization of the gabbroic magma.

The significance of the younger concordant dates is unknown. Nearly all 31 analyses have alpha doses (calculated at 2150 Ma) well below that of Stage 1 defined by Murakami et al. (1991), thus it is likely that they represent new zircon growth rather than Pb loss. Unfortunately, we were not able detect any growth zoning in the CL images and we cannot exclude the possibility that these younger dates represent mixed analyses between ca. 2150 Ma domains and younger zircon (e.g., formed during ca. 1900 Ma Svecofennian metamorphism). More work is required to resolve this. In either case, the low alpha doses make it unlikely that the older concordant population has been significantly affected by Pb loss. The 2156 Ma age of the intrusion provides a minimum depositional age constraint for the Gollebáiki Formation.

4.4.2. Quartz-diorite dike

A c. 1 m-thick quartz-diorite dike intrudes the upper part of the Gollebáiki Formation. The sample (2018-HAH-075) is massive, unfoliated and fine-grained quartz-diorite with < 1 mm plagioclase phenocrysts and < 0.4 mm quartz grains. Minor phases are magnetite and ilmenite (Figs. 8I and J). Zircons are euhedral, elongated, prismatic

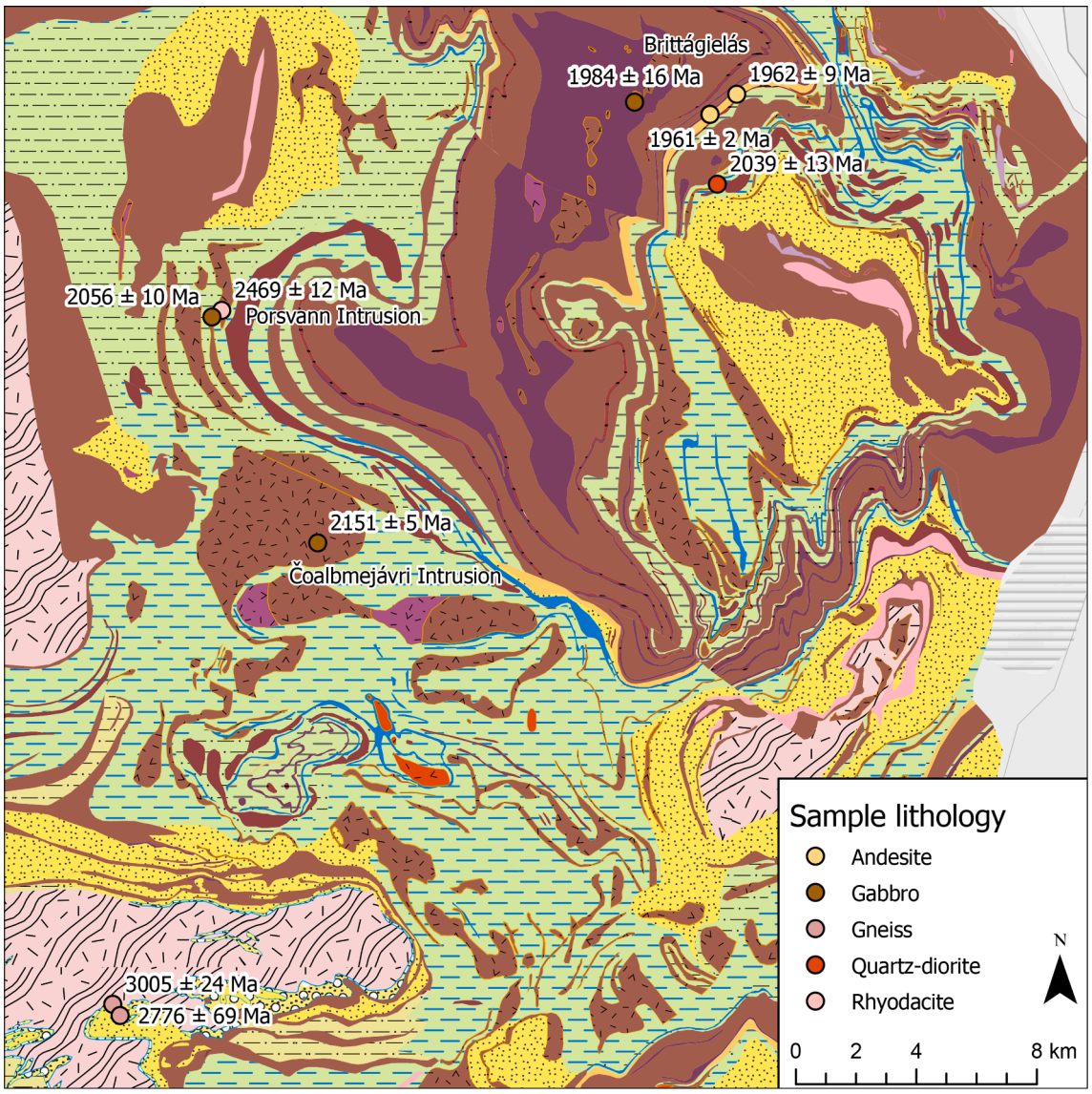

Fig. 6. Geochronological results from northern Karasjok Greenstone Belt. See Fig. 2 for lithological legend and location of the study area. Coordinates for samples are given in Table 1.

crystals between 100 and 200 μm in size. They show weak oscillatory zoning in CL. Twenty-four analyses define upper and lower intercept dates of 2039 ± 13 and 287 ± 27 Ma, respectively (MSWD = 1.5, Fig. 10C). The upper intercept date is interpreted as the crystallization age of the dike.

4.5. *Báhkilvárri Formation*

The Báhkilvárri Formation lies on the Gollebáiki Formation and mainly consist of volcanic lithologies. Two volcanic units from this formation were dated.

4.5.1. *Fossestrand Member*

The komatiites of the Fossestrand Member are in the lower part of the Báhkilvárri Formation (Fig. 3). The komatiitic flows and tuffaceous extrusive units alternate with pyroxenitic and gabbroic intrusions. Sample *2018-HAH-029* (Fig. 7E) is from a gabbroic intrusion in the Fossestrand Member from the northern part of the study area (Fig. 6). The intrusion is interpreted to be synvolcanic and thus provides an age for the komatiites. The sample comes from a metagabbronorite and consists of amphibole pseudomorphs after pyroxenes, intercumulus plagioclase, chlorite, and serpentine (Figs. 8K and 8L). The zircons are elongated, 100–200 μm in length with prismatic crystal faces. Most of the grains have a chaotic core with inclusions of titanite or a weak oscillatory zoning in CL. Excluding three analyses with high common Pb, the remaining 28 analyses define a discordia with rather imprecise upper and lower intercept dates of 2024 ± 45 and 360 ± 45 Ma (MSWD = 180, Fig. 10D). Eleven analyses that are < 12% discordant form a cluster close to concordia and yield a weighted average $^{207}Pb/^{206}Pb$ date of 1984 ± 16 Ma (MSWD = 39, Fig. 10E), within the uncertainty of the upper intercept date and interpreted as the best estimate of the crystallization age of the gabbro.

4.5.2. *Andesitic volcanics*

We analyzed three samples from a distinct 50–70 m-thick unit of andesitic volcanics in the upper part of the Báhkilvárri Formation (Figs. 3 and 6). It is a fine- to medium-grained, light-gray, compositionally layered, strongly foliated volcanic unit and it contains layers with massive sulfides (Fig. 7F; Davidsen, 1994; Roberts and Davidsen, 2011; Siedlecka et al., 2011). The unit is dominated by plagioclase, biotite, and amphibole. Minor phases are chlorite, titanite, epidote, and sulfides (Figs. 8M and 8N). Most zircons extracted by heavy mineral

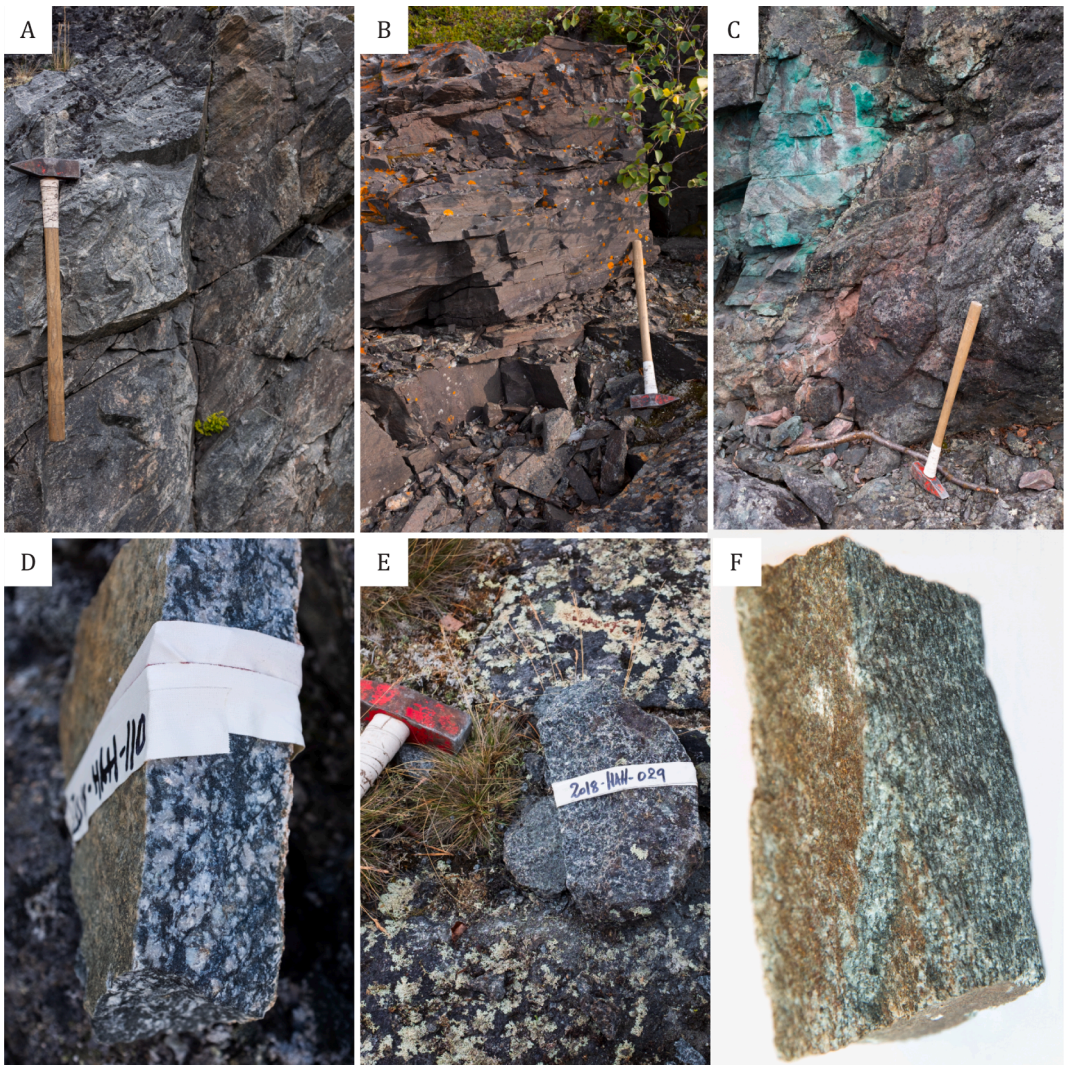

Fig. 7. A) Migmatitic gneiss from the Jergul Gneiss Complex (sample 2018-HAH-103). **B)** Rusty red-colored rhyolitic metavolcanite (leptite) from the Vuomagielas Formation (2018-HAH-100). **C)** Anorthositic lens in contact with Cu-PGE mineralization in the Porsvann Intrusion (2018-HAH-098) **D)** Metagabbro from the Čoalbmejávri Intrusion (Sample 2018-HAH-110). **E)** Metagabbronorite from the Fossestrand Member in the Báhkilvárri Formation (2018-HAH-029). **F)** Andesitic volcanite from the Báhkilvárri Formation. Specimen is 2.5 cm thick (2019-HAH-112).

separation are 100–200 μm in size and euhedral in shape. They show oscillatory zoning from core to rim in CL.

Five analyses from sample 2019-HAH-112 were identified as containing common Pb and the remaining 26 analyses yield a poorly defined discordia with upper and lower intercept dates of 1976 ± 14 and 221 ± 140 Ma, respectively (MSWD = 11.4, Fig. 11A). The majority (20) of the analyses are < 10% discordant and yield a weighted mean $^{207}Pb/^{206}Pb$ date of 1961 ± 2 Ma (MSWD = 1.7, Fig. 11B, one analysis identified as a statistical outlier by Isoplot), interpreted to represent the crystallization age of the volcanic rock.

Excluding two analyses with high common Pb, the remaining 22 analyses from sample 2018-HAH-021 yield a discordia with upper and lower intercept dates of 1962 ± 11 and 29 ± 79 Ma, respectively (MSWD = 0.73, Fig. 11C). The former is interpreted to represent the crystallization age of the volcanic rock, whereas the latter most likely represents recent Pb loss.

Twenty-four analyses from the third sample of the same lithology (2018-HAH-050) yield a discordia with upper and lower intercept dates of 1952 ± 11 and 12 ± 150 Ma, respectively (MSWD = 1.02, Fig. 11D). The former is interpreted to represent the crystallization age of the volcanic rock, whereas the latter most likely represents recent Pb loss. The weighted average $^{207}Pb/^{206}Pb$ date of analyses with < 5% discordance from all three samples is 1961 ± 1 Ma (MSWD = 2.3), which is considered to be the best estimate of the age of volcanism during deposition of the upper part of the Báhkilvárri Formation.

5. Stable isotope data for the KGB carbonates

Considering that some carbonate beds are impure, with low carbonate content, and that they experienced amphibolite facies metamorphism and thermal metamorphism at the contact with intrusions, the samples with the highest C and O isotope values and carbonate content are taken as most likely to be representative of primary or near-to-primary carbonate and seawater C isotope composition. Indeed, all post-depositional, late diagenetic to metamorphic processes, tend to lower C and O isotope values in carbonates (e.g., Valley, 1986; Valley, 2001; Baumgartner and Valley, 2001; Satish-Kumar et al., 2021).

The isotope data (Table 2) show that all samples from the Skuvvánvárri and Gollebáiki formations have elevated $\delta^{13}C$ values. $\delta^{13}C$ values range from + 3.7 to + 4.1 ‰ for the Skuvanvarri Formation samples, regardless of the degree of recent weathering (compare data for the KGB-05 and KGB-06 samples with that for the KGB-07 sample), potentially indicating deposition of this unit at the early stage of the LCIE, when C isotope values of seawater dissolved inorganic carbon

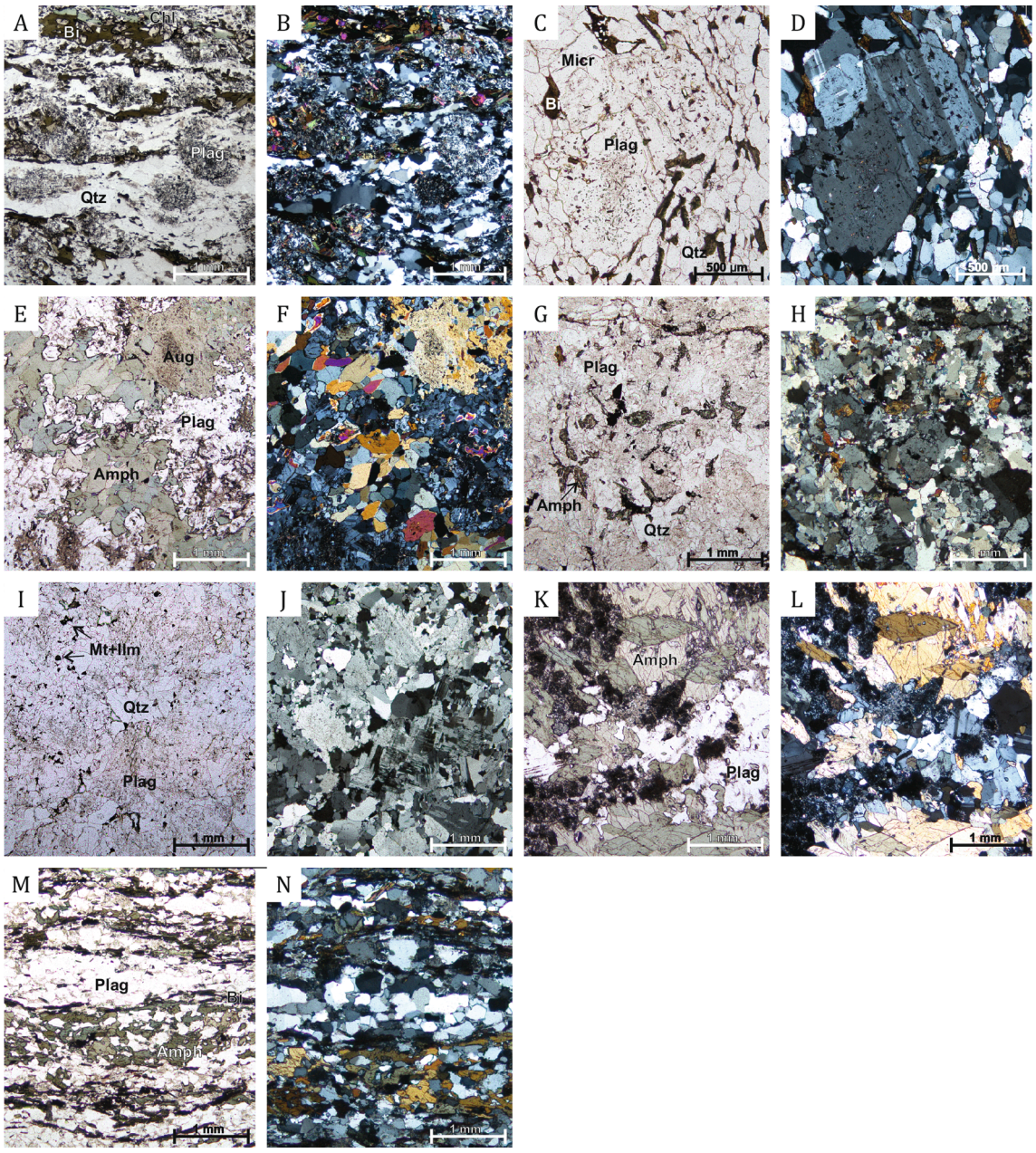

Fig. 8. Photomicrographs of selected samples from the Jergul Gneiss Complex and KGB units (see Table 1). **A)** Sample 2018-HAH-103 of Jergul gneiss in plane-polarized light (PP), showing almost completely sericitized porphyroblasts of plagioclase in a matrix of fine-grained quartz. Layers of biotite and minor chlorite define the foliation. **B)** Sample 2018-HAH-103 in cross-polarized (XP) light. **C)** Rhyolitic volcanite (leptite) from the Vuomegielas Formation. Plagioclase phenocryst in groundmass of quartz, microcline, and biotite. (Sample 2018-HAH–100 in PP). **D)** Sample 2018-HAH–100 in XP. **E)** Metagabbro from the Čoalbmejávri Intrusion. Plagioclase, enstatite, green secondary amphibole, and remnants of partly metamorphosed augite (Sample 2018-HAH–110 in PP). **F)** Sample 2018-HAH–110 in XP. **G)** Anorthositic interlayer from the Porsvann Intrusion. Hematite-stained plagioclase with interstitial quartz and amphibole (Sample 2018-HAH-098). **H)** 2018-HAH-098 in XP. **I)** Fine-grained quartz-dioritic vein from the Gollebáiki Formation (2018-HAH-075). Plagioclase and smaller quartz grains with minor interstitial magnetite and ilmenite. **J)** 2018-HAH-075 in XP. **K)** Metagabbro from the Fossestrand Member in PP. Amphiboles replacing magmatic pyroxene. Intercumulus plagioclase, partly seriticized and hematite stained. Minor phases are chlorite and serpentine (2018-HAH-029). **L)** 2018-HAH-029 in XP. **M)** Banded andesitic volcanics from the Báhkilvárri Formation. Granoblastic plagioclase with layers of amphibole showing green pleochroism and biotite (2018-HAH-021) in PP. **N)** 2018-HAH-021 in XP. Mineral abbrevations: Qtz = quartz, Micr = microcline, Bi = biotite, Plag = plagioclase, Amph = amphibole, Mt = magnetite, Ilm = ilmenite, Chl = chlorite.

were rising to the peak of the LCIE. Carbonates of the Gollebáiki Formation (Table 2) show a large range of C isotope values up to + 12.5 ‰, consistent with their deposition during the peak of the LCIE. By contrast, the carbonate sample from the Bahkilvárre Formation displays a near-to-zero $\delta^{13}C$ value of + 1.4 ‰, typical for marine carbonates deposited in the aftermath of the LCIE (Bekker et al., 2003; Bekker, 2022).

6. Discussion

The U-Pb zircon dating results presented above provide more detailed and precise geochronological constraints for the stratigraphy of the KGB than was previously available (e.g., Krill et al., 1985). Our data indicate the presence of Archean (3.0–2.8 Ga) basement rocks below the KGB volcanosedimentary and intrusive sequence in the Lakselv area,

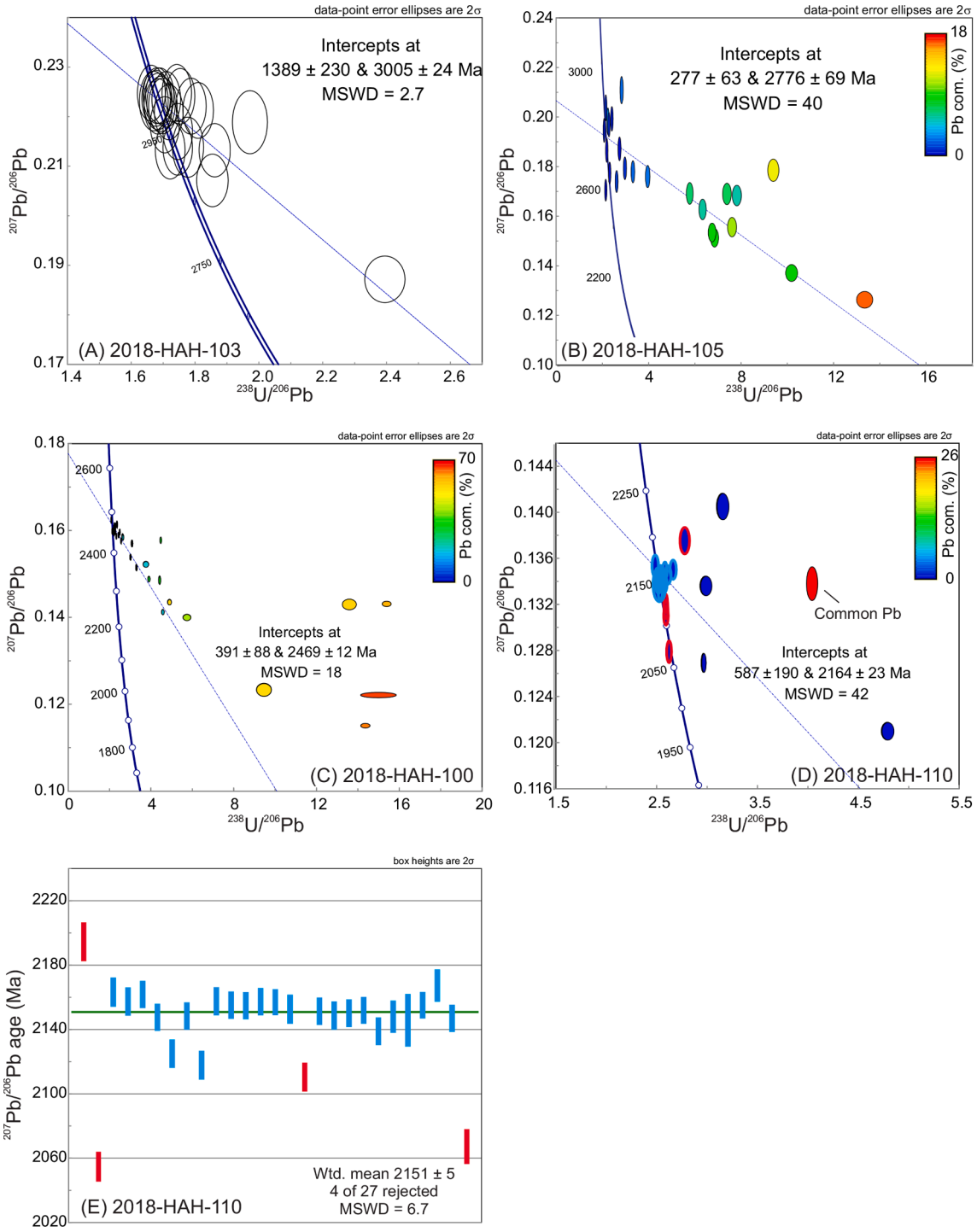

Fig. 9. Zircon U-Pb results from the Jergul Gneiss Complex and Karasjok Greenstone Belt plotted in Tera-Wasserburg concordia diagrams. CL and BS images of analyzed zircons are found in electronic supplement B. Ellipses in (B), (C), and (D) are colored according to percentage of common Pb, see text for calculation procedure. **A)** Heterogeneous and partly migmatitic Jergul gneiss from basement window north of Skoganvárre (Sample 2018-HAH-103). **B)** Jergul gneiss from tectonic window north of Skoganvárre (Sample 2018-HAH-105). Oldest measurement gives a concordia age of 2818 ± 15 Ma, the youngest is 2599 ± 15 Ma. **C)** Rhyodacite from the Vuomegielas Formation taken north of Porsvann (Sample 2018-HAH-100). Discordia calculated for 17 analyses without identifiable common Pb, black ellipses. **D)** Metagabbronorite from the Čoalbmejávri Layered Intrusion (2018-HAH-110). Ellipses with blue rims included in weighted average age calculation, red rims indicate analyses identified as statistical outliers by Isoplot. **E)** Weighted average plot of analyses from sample 2018-HAH-110 that are < 10% discordant. Blue bars included in calculated age, red bars excluded by Isoplot as statistical outliers.

which spans the time interval from c. 2.46 Ga to 1.96 Ga. The entire KGB thus formed during a period of major extension and supercraton breakup in Fennoscandia (Lahtinen et al., 2008; Bingen et al., 2015; Lahtinen and Köykkä, 2020), resulting in development of rift basins and deposition on a passive continental margin. The KGB also corresponds to a period of rapid increase in atmospheric oxygen and a major change in the global carbon cycle, i.e., the c. 2.3–2.05 Ga LCIE (Martin et al., 2013; Bekker, 2022). Below, we discuss wider implications of the new geochronologic and chemostratigraphic data, focusing on the tectonic setting, evolution, and depositional history of the KGB, and possible correlations with other

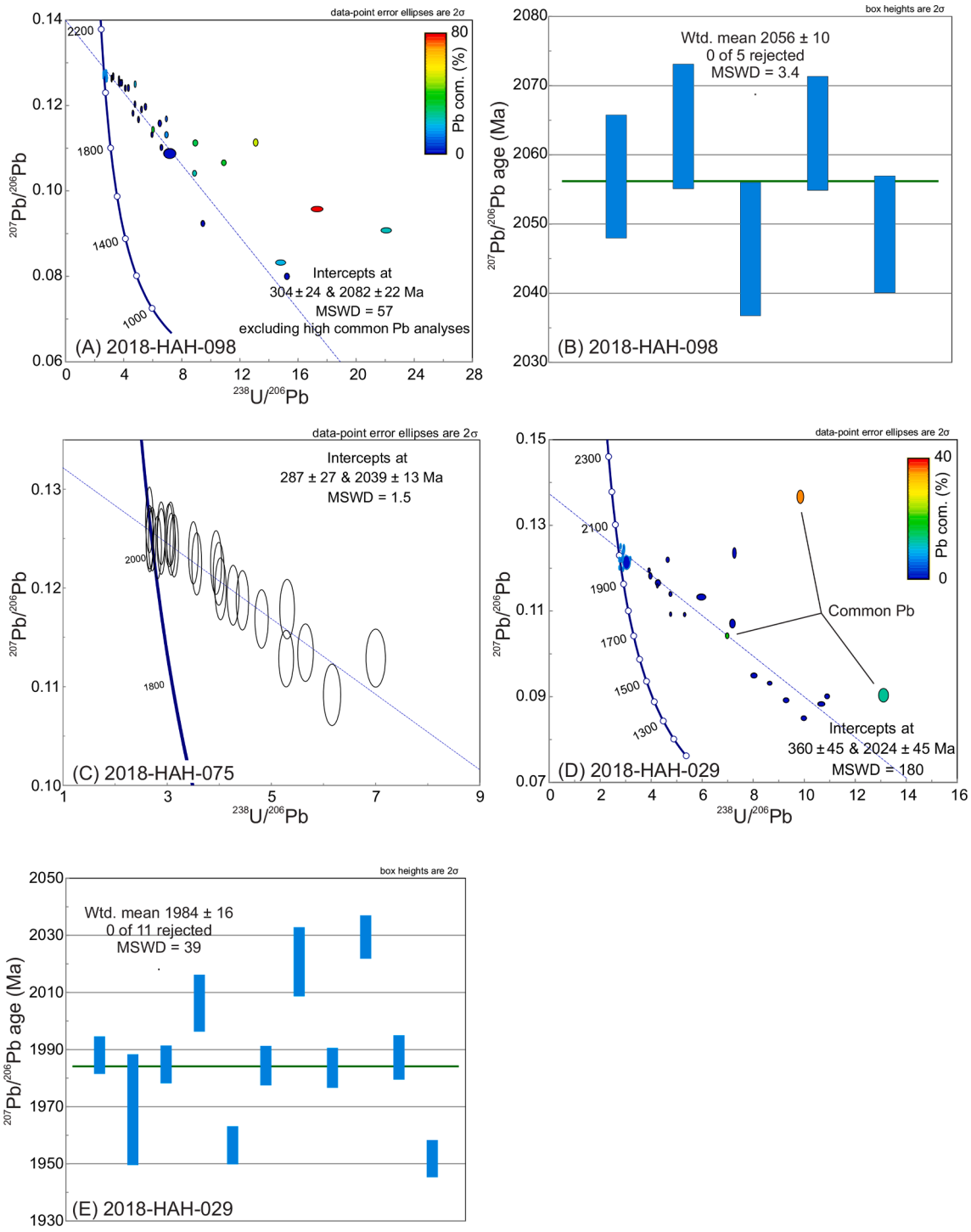

Fig. 10. Zircon U-Pb results from magmatic lithologies in the Skuvvanvárri, Gollebáiki, and Báhkilvárri formations plotted in Tera-Wasserburg concordia diagrams. CL and BS images of analysed zircons are found in electronic supplement B. Ellipses in (A) and (D) are colored according to percentage of common Pb, see text for calculation procedure. **A)**Sample of anorthositic interlayer from the Cu-PGE mineralized outcrop in the Porsvann intrusion (2018-HAH-098). Blue ellipses do not contain identifiable common Pb and were included in the regression. **B)** Weighted average plot of analyses from 2018-HAH-098 that are $< 6\%$ discordant. **C)** Quartz-diorite dike from the Báhkilvárri Formation (2018-HAH-075). **D)** Metagabbro from the Fossestrand Member (2018-HAH-029). Blue ellipses do not contain identifiable common Pb and were included in the regression. **E)** Weighted average plot of analyses from sample 2018-HAH-029 that are $< 12\%$ discordant.

supracrustal belts on the northern Fennoscandian Shield (Figs. 3 and 12).

6.1. *Correlation of Archean units on the northern Fennoscandian Shield*

The gneiss sample taken from the tectonic window at Skoganvárre (*sample 2018-HAH-103*) gave a U-Pb zircon date of 3005 ± 24 Ma (Table 1 and Fig. 9A). The second sample from the same tectonic window (*2018-HAH-105*) gave a more ambiguous result as the most concordant analyses spread out along concordia with 2818 ± 15 Ma to 2599 ± 15 Ma (Fig. 9B). This suggest that this sample either represents a paragneiss (i.e., the zircons are detrital), or late Archean partial to

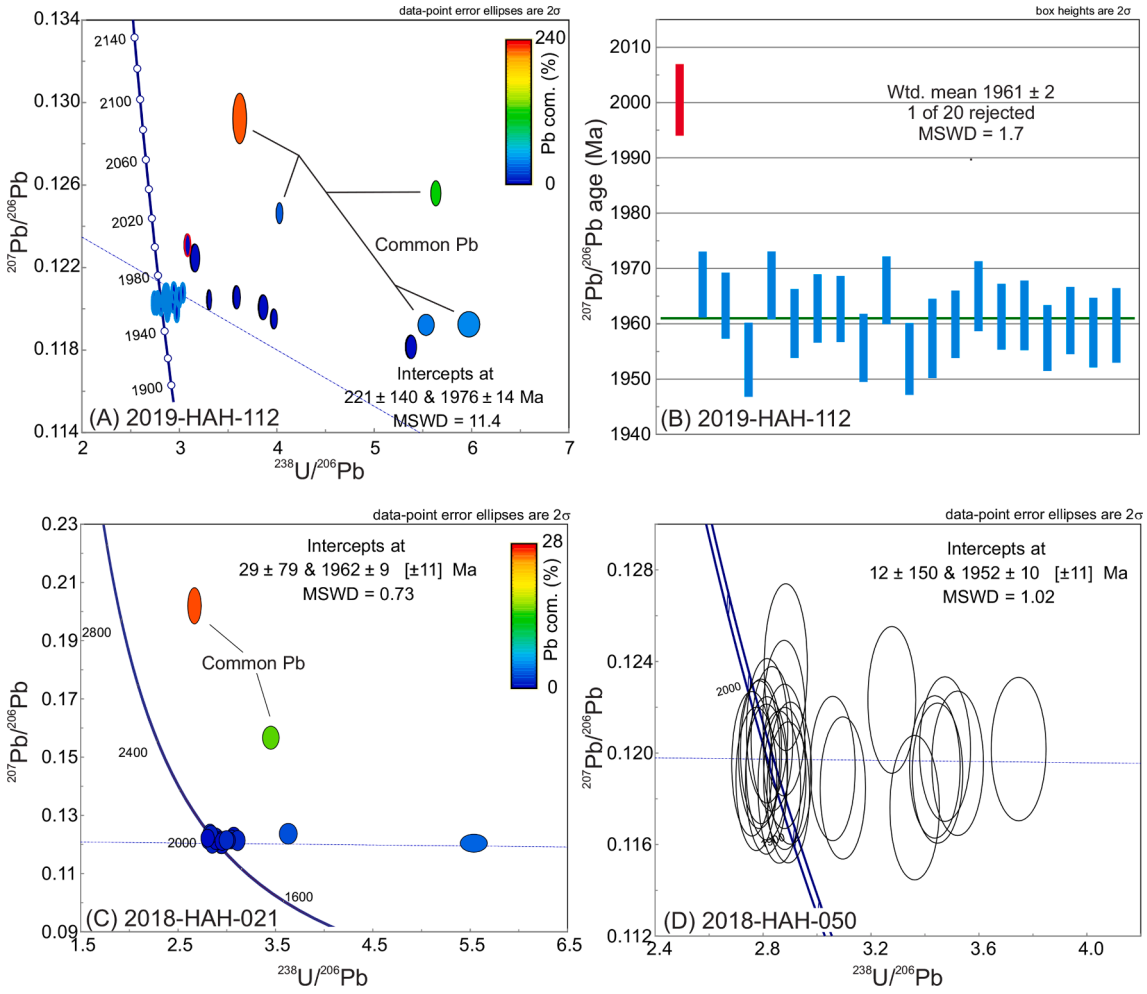

Fig. 11. Zircon U-Pb results from andesitic volcanites from the upper part of the Báhkilvárri Formation plotted in Tera-Wasserburg concordia diagrams. CL and BS images of analysed zircons are found in electronic supplement B. Ellipses in (A) and C) are colored according to percentage of common Pb, see text for calculation procedure. **A)** Sample 2019-HAH-112. Ellipses with blue rims included in weighted average age calculation, red rims indicate analyses identified as statistical outliers by Isoplot. **B**Weighted average plot of analyses from sample 2018-HAH-112 that are < 10% discordant. Blue bars included in calculated age, red bars excluded by Isoplot as statistical outliers. **C)** Sample 2018-HAH-021 **D)** Sample 2018-HAH-050.

complete isotopic resetting during metamorphism. The latter interpretation would indicate a magmatic age of the gneiss in excess of 2818 Ma and a metamorphic event at c. 2600 Ma. A metamorphic event with this age is recorded in Lofoten and Vesterålen (Griffin et al., 1978; Corfu, 2007), the West Troms Basement Complex (Myhre et al., 2013), and farther south in the Norrbotten Province (Slagstad et al., 2015).

Farther west in the Jergul Gneiss Complex Bingen et al. (2015) reported ages between 2975 Ma and 2776 Ma, which have the same age range as our samples from Skoganvárre. This suggests that both the western and eastern parts of the Jergul Gneiss Complex belong to the same Archean TTG unit. Further, the presence of TTG gneisses with a similar age in tectonic windows inside the KGB indicates that the KGB was deposited in a rift setting on the same continental crust and does not represent an exotic allochthon or contain ophiolites.

The age of the Archean Goldenvárri Formation is bracketed between 2833 ± 4 Ma and 2781 ± 4 Ma (Bingen et al., 2015). This suggests that parts of the eastern Jergul Gneiss Complex are coeval with or slightly younger than the rifting event that resulted in deposition of the Goldenvárri Formation.

The West Troms Basement Complex (Fig. 1) contains similarly aged Archean gneisses. The c. 2.92–2.80 Ga tonalitic gneiss basement and the associated c. 2.85 Ga Ringvassøy Greenstone Belt are the oldest lithotectonic segments of the West Troms Basement Complex (Bergh et al., 2010; Bergh et al., 2014). Myhre et al. (2013). In addition, there is a younger segment of granitoids to the south in the West Troms Basement Complex with a time span of 2.74–2.67 Ga (Laurent et al., 2019). This range of ages is similar to that observed in the KGB and strengthens the interpretation that the West Troms Basement Complex is a part of the Karelian craton and that both regions formed in coeval and similar tectonic regimes. A similar range of ages has been obtained for the Altevatn area in the eastern Troms and the Mauken window in central Troms (Bjerkgård et al., 2015; Slagstad et al., 2015), suggesting that continental crust of this age underlies the Caledonian nappes in Troms and Finnmark.

The 3005 ± 24 Ma age for sample 2018-HAH-103 from the Skoganvárre tectonic window overlaps within uncertainty the 2975 ± 10 Ma age for a granitic gneiss from the Vuottašjávri borehole in the western part of the Jergul Gneiss Complex (Bingen et al., 2015). Isotopic data for the KGB suggest evidence for even older basement at depth (Orvik et al., 2022). The oldest unit that so far has been identified on the Fennoscandian Shield is the c. 3.5 Ga Siurua trondhjemite gneiss in the Pudasjärvi Granulite Belt, northern Finland (Mutanen and Huhma, 2003; Lauri et al., 2011).

6.2. *The c. 2.45 Ga Sumian period: onset of protracted rifting on the Fennoscandian Shield*

The 2469 ± 12 Ma age for the rhyodacites from the upper

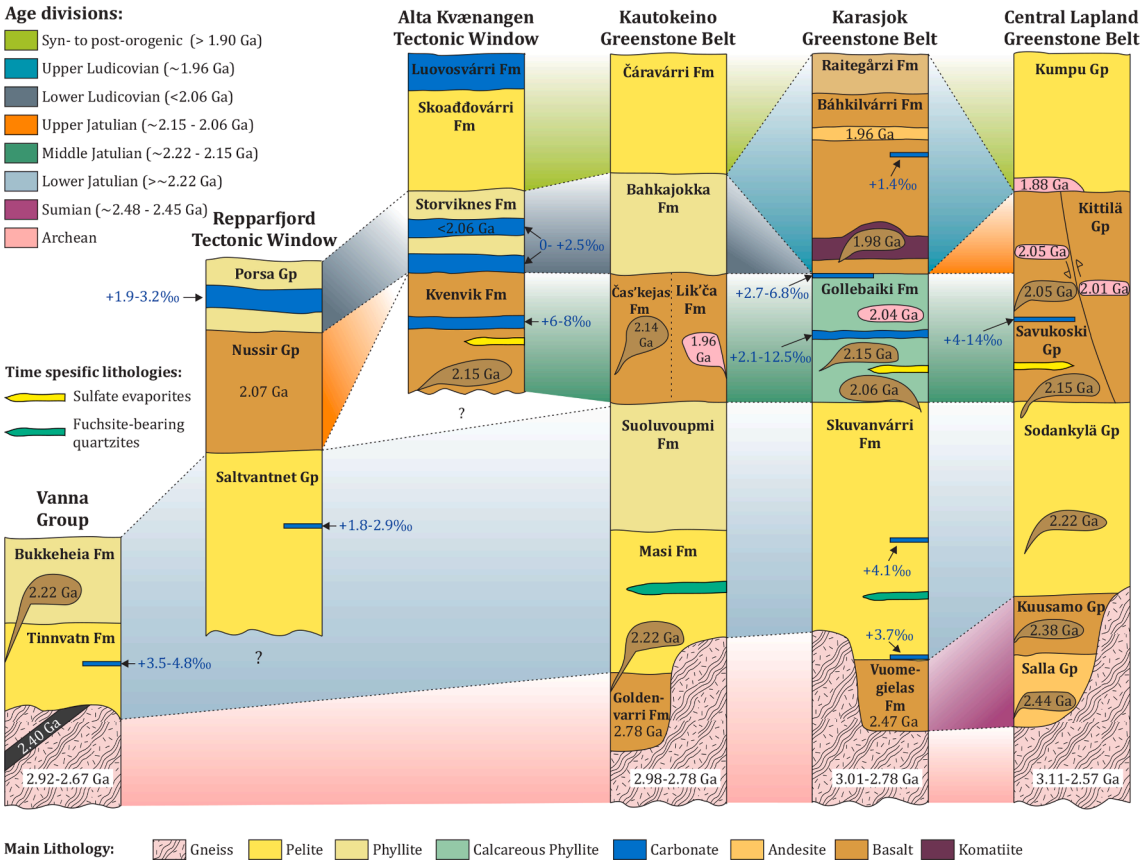

Fig. 12. Simplified stratigraphic columns showing stratigraphy and correlations for the supracrustal belts in northern Fennoscandia, based on the U–Pb zircon dating in the KGB presented herein. Blue numbers show $\delta^{13}C$ values from carbonates. Data from: Vanna Group: Bergh et al. (2007); Paulsen et al. (2021); Johannesen (2012), Repparfjord Tectonic window: Pharaoh et al. (1983); Torgersen et al. (2015); Mun et al. (2020), Alta–kVænangen Tectonic Window: ZZwaan and Gauthierwaan and Gauthier (1980); Melezhik et al. (2015), Kautokeino Greenstone Belt: Siedlecka (1985); Solli (1983); Bingen et al. (2015), Karasjok Greenstone Belt: Siedlecka (1985); Braathen and Davidsen (2000), Central Lapland Greenstone Belt: Hanski and Huhma (2005); Huhma et al. (2018); Haverinen (2020).

Vuomegielas Formation in the KGB shows that this unit is a part of the *Sumian* system (2505–2430 Ma; Hanski and Melezhik, 2013). It is coeval with widespread bimodal magmatism, including layered mafic intrusions, intracratonic granitic intrusions, and ultramafic to felsic volcanism, that is typical for this period on the Fennoscandian Shield (Amelin et al., 1995; Lauri and Mänttäri, 2002; Lauri et al., 2012).

The 2505–2430 Ma magmatism on the Fennoscandian Shield is related to protracted rifting of the Superia supercraton during the Archean to Paleoproterozoic transition. This time period is globally characterized by episodic crustal rifting and large igneous provinces emplaced by mantle plumes, including bimodal magmatism, dike swarms, and thick volcanic accumulations (Heaman, 1997; Vogel et al., 1998; Ernst and Bleeker, 2010; Söderlund et al., 2010; Ciborowski et al., 2015; Gumsley et al., 2017; Zakharov et al., 2022). The 2450–2430 Ma magmatism on the Karelia and Kola cratons correlates well with the Matachewan mantle plume event, which plume center is thought to be located at the southern tip of the Superior craton. This event formed a rift system with propagating rift arms, rift volcanism, and dike swarms, but did not result in a full-scale break-up of the supercontinent (e.g., Ernst and Bleeker, 2010; Söderlund et al., 2010; Ciborowski et al., 2015).

The age of the Vuomegielas Formation matches well with the lowermost Salla Group of the Central Lapland Greenstone Belt (Fig. 12; Hanski and Huhma (2005)), which was deposited under subaerial conditions. By comparison, a felsic tuff from the Salla Group in the Rookkiaapa Formation yields an age of 2426 ± 6 Ma (Manninen et al., 2001; Huhma et al., 2018), and a dacitic metavolcanic rock at Sakiamaa yields an age of 2438 ± 11 Ma (Räsänen and Huhma, 2001).

Köykkä et al. (2022) interpreted the *Sumian* volcanism in the Salla Group and coeval units on the Karelian craton to represent a rift arm radiating away from the plume center. The KGB could then represent the northwestern extension of this system. The age and paleogeographic setting of the Vuomegielas Formation in the northern KGB therefore support a scenario where the mantle plume propagated from the north and initiated first magmatism and early rifting in the northern part of the Karelian and Kola cratons while it continued to progress southeastwards.

6.3. *The early Jatulian (c. 2.22 Ga) carbon isotope excursion*

The exact depositional age of the Skuvanvárri Formation of the KGB is unknown, but the presence of abundant, green-colored fuchsite in the metapsammites suggest a correlation with the early Jatulian Masi Formation in the Kautokeino Greenstone Belt (Siedlecka et al., 1985; Braathen and Davidsen, 2000). Bingen et al. (2015) obtained a U-Pb zircon age of 2220 ± 7 Ma for an albite diabase sill, which intruded the Masi Formation. This age defines a minimum age for deposition of the Masi Formation and potentially Skuvanvárri Formation. Given that the correlation between the two formations is correct, the Skuvanvárri Formation was deposited between 2460 ± 12 Ma, the age of the underlying Vuomegielas Formation, and 2220 ± 7 Ma. The source of chromium needed for the fuchsite-bearing basal units of the Skuvanvárri Formation could be the ultramafic volcanic rocks of the Vuomegielas Formation and/or the Archean Goldenvárri Formation, which partially covered the Jergul Gneiss Complex.

Further constraints on the depositional age of the Skuvanvarri

Formation are provided by the elevated $\delta^{13}C$ values of carbonates from this unit ranging between + 3.7 and + 4.1 ‰ (Table 2). This indicates that the calcareous sediments were likely deposited after the onset of the LCIE (Martin et al., 2013; Bekker, 2022).

The Sodankylä Group of the Central Lapland Greenstone belt is a continuation of the Skuvanvárri Formation southward into Finland. Its basal contact resembles that of the Skuvanvárri Formation, where the alluvial clastic sediments were either deposited on the Archean basement or conformably on the underlying Salla and Kuusamo Group volcano-sedimentary units (Fig. 12). The depositional age of the group is between c. 2.35–2.33 Ga (age of youngest detrital zircons; Köykkä et al., 2019) and 2213 ± 14 Ma (zircon Pb-Pb age of intruding mafic sills; Huhma et al., 2018). Carbonates of the Sodankylä Group record the rising trend in carbon isotope values up to >10 ‰, likely corresponding to the peak of the LCIE (Karhu, 1993) and contain sulfate evaporites.

The Vanna Group (c. 2.4–2.2 Ga) in the West Troms Basement Complex (Bergh et al., 2007) is another coeval, siliciclastic, metasedimentary succession in the northwestern part of the Fennoscandian Shield that might correlate with the Skuvanvárri and Masi formations. It consists of well-preserved fluviodeltaic sandstones and calcareous phyllites deposited in a subsiding rift basin (Paulsen et al., 2021). Calcareous phyllites on Vanna have C isotope values ranging between + 3.2 and + 4.8‰ (Johannesen, 2012), which are similar to those of carbonates from the Skuvanvarri Formation.

In summary, the depositional age of all these successions is bracketed between c. 2.35/2.32 and 2.22 Ga, and commonly taken to be closer to c. 2.22 Ga (eg., Köykkä et al., 2019). Alternatively, they could be closer in their depositional age to c. 2.31 Ga and, in this case, they would correlate with the c. 2.31 Ga Gordon Lake Formation of the Huronian Supergroup on the Superior craton that records the LCIE and also contains sulfate evaporites (Bekker et al., 2005; Rasmussen et al., 2013).

6.4. The mid-Jatulian (c. 2.16 Ga) Gollebáiki Formation records the peak of the LCIE

A *Jatulian* (c. 2.16 Ga) age is proposed for the Gollebáiki Formation, based on an estimated minimum depositional age provided by the 2151 ± 5 Ma Čoalbmejávri intrusion. The maximum age is only limited by the inferred depositional age of the Skuvanvárri Formation (c. 2350/2320–2220 Ma). If we assume that the Gollebáiki Formation basalts are synmagmatic with the oldest generation of intrusions in the formation, then the age of the formation is c. 2151 Ma. This age corresponds with the rifting and continental breakup events that led to the emplacement of one of the most widespread Paleoproterozoic Large Igneous Provinces (LIPs) on the Fennoscandian Shield (e.g. Lahtinen et al., 2008; Hanski, 2013).

The 2151 Ma magmatism also corresponds to the opening of the Kola and Svecofennian oceans (i.e. Lahtinen et al., 2008), in a period of rising atmospheric oxygen and the LCIE (Martin et al., 2013; Bekker and Holland, 2012; Bekker, 2022). A rift-to-drift transition is supported by the presence of subaqueous volcanics, coastal to marine sediments, sulfate evaporites, and stromatolitic carbonate reefs in temporally correlative volcanosedimentary succesions in Fennoscandia (Hanski and Melezhik, 2013). The highly positive $\delta^{13}C$ isotope values, up to + 12.5 ‰, of the Gollebáiki Formation carbonates (Table 2) indicate that the carbonates and calcareous sediments were deposited after the onset and likely at the peak of the LCIE.

Possible correlative units to the Gollebáiki Formation are the Čáskejas and Likčá formations of the Kautokeino Greenstone Belt, where a synvolcanic gabbro yielded an age of 2137 ± 5 Ma (Bingen et al., 2015). Farther west in the Alta-kVænangen tectonic window, a gabbro synmagmatic with the tholeiitic volcanics-dominated Kvenvik Formation (Bergh and Torske, 1988) yields the 2146 ± 5 Ma U-Pb zircon age, which is the same within analytical uncertainty as that for the gabbro of the Caskejas Formation (Melezhik et al., 2015). The Kvenvik Formation carbonates have positive $\delta^{13}C$ values, ranging between + 6 and + 8.5 ‰ (Melezhik et al., 2015).

The 2148 ± 11 Ma Rantavaara gabbro hosted in black schists of the lower Savukoski Group in the Central Lapland Greenstone Belt (Fig. 12) provides a similar minimum age for this unit to that of the Gollebáiki, Caskejas, and Kvenvik formations (Räsänen and Huhma, 2001; Huhma et al., 2018). Carbonates of the Savukoski Group record an upward stratigraphic decrease in carbon isotope values ~10 ‰ down to ~0 ‰, corresponding to the end of the LCIE (Karhu, 1993). The Savukoski Group could thus cover the mid-Jatulian to early Ludicovian transition.

Magmatism of the Gollebáiki Formation of the KGB is also coeval with MORB-type tholeiitic dikes developed further away, in southeastern Karelia (Stepanova et al., 2014) and in the Belomorian Province in the eastern part of the Fennoscandian Shield (Stepanova and Stepanov, 2010).

6.5. Early Ludicovian (c. 2.07–2.04 Ga) magmatism

The 2056 ± 10 Ma age for the Ni-Cu-PGE-mineralized Porsvann layered intrusion and the overlapping 2051 ± 8 Ma age for the similarly mineralized Gallujavri intrusion (Orvik et al., 2022), both hosted in the Skuvanvárri Formation, and the 2039 ± 13 Ma age for a quartz-dioritic dike in the upper part of the Gollebáiki Formation show that they all formed during the earliest *Ludicovian* time period (c. 2.07–2.04 Ga) (Mutanen and Huhma, 2001; Hanski et al., 2001). This magmatism corresponds to a period of continued rifting and continental breakup on the Superia supercraton (Bekker and Eriksson, 2003; Kilian et al., 2015; Kilian et al., 2016; Mammone et al., 2022).

In the Central Lapland Greenstone Belt, a 2058 ± 4 Ma U-Pb zircon age and a 2063 ± 35 Ma Re-Os age were obtained for the Kevitsa and Sakatti mafic–ultramafic intrusions, respectively, hosted by the Savukoski Group (Fig. 10; Mutanen and Huhma, 2001; Moilanen et al., 2021). These ages suggest that magmatic Ni-Cu-PGE deposits in the KGB and Central Lapland Greenstone Belt are coeval and tightly define the age of these deposits. The 2039 ± 13 Ma age for the quartz-dioritic dike hosted in the Gollebáiki Formation of the KGB appears to be slightly younger (but overlaps within analytical uncertainty) than the most voluminous early *Ludicovian* magmatic event responsible for the Ni-Cu-PGE-bearing intrusions and komatiites, but contemporaneous with the Moskuvaara (2039 ± 14 Ma Pb-Pb zircon age) and the Puijärvi (2035 ± 8 Ma Pb-Pb zircon age) gabbros hosted in the Savukoski Group and the Satovaara gabbro (2025 ± 8 Ma Pb-Pb LA-ICP-MS age); all three developed in the Central Lapland Greenstone Belt (Huhma et al., 2018).

Other potentially correlative igneous units to the Ludicovian mafic to ultramafic KGB intrusions include the Jeesiörova komatiites and Peuramaa picrites of the adjacent Kittilä Greenstone Belt that yield a Sm-Nd clinopyroxene and whole-rock isochron age of 2056 ± 25 Ma (Hanski et al., 2001). The Kevitsa komatiitic dikes of the Central Lapland Greenstone Belt and the Jeesiörova komatiites yield a Re-Os isocron age of 2049 ± 13 Ma (Puchtel et al., 2020). Farther east, in the Imandra-Varzuga and Pechenga Greenstone Belts of Russia, mafic volcanic units and tuffs, deposited after the end of the LCIE, yield a U-Pb zircon age of 2057 ± 1 Ma (Melezhik et al., 2007; Martin et al., 2013).

Ludicovian volcanic rocks are also present farther west of the KGB, in the Repparfjord Tectonic Window, where the Nussir Group contains coeval volcanic rocks with U–Pb zircon ages of 2073 + 23/-12 Ma (Perello et al., 2015), but these magmatic events have so far not been identified in the Kautokeino Greenstone Belt and the Alta-kVænangen Tectonic Window (Bingen et al., 2015; Melezhik et al., 2015).

Carbonates of the Storviknes Formation of the Alta-kVænangen Tectonic Window and the Porsa and Saltvatnet groups of the Repparfjord Tectonic Window, respectively overlying and underlying the Nussir Group, have C isotope values close to 0 ‰ (Melezhik et al., 2015; Torgersen et al., 2015; Mun et al., 2020), typical for the aftermath of the LCIE (Bekker et al., 2003; Melezhik et al., 2007; Bekker, 2022).

6.6. The late Ludicovian (c. 1.98–1.96 Ga) period of terminal rifting

The 1984 ± 16 Ma U-Pb zircon age for the synvolcanic gabbro in the Fossestrand Member of the Báhkilvárri Formation is interpreted to reflect the time of emplacement of the komatiitic lavas in the area. This implies that there was another so far unrecognized late *Ludicovian* pulse of komatiitic magmatism on the northwestern Fennoscandian Shield more than 50 million years after the c. 2.05 Ga event, although we note that further work is needed to verify this age due to potentially disturbed U-Pb systematics The intermediate volcanic rocks in the upper part of the formation collected from the same volcanic units, but at different locations, yield a combined U-Pb zircon age of 1961 ± 1 Ma, indicating that this magmatic event potentially lasted for more than 10 million years.

Notably, the sampled carbonates of the Báhkilvárre Formation yield a near-to-zero $\delta^{13}C$ value (∼1.4 ‰) which is much lower than those for the Jatulian Skuvanvarri and Gollebáiki formations (Table 2). The LCIE ended by c. 2.06 Ga (Bekker et al., 2003; Melezhik et al., 2007; Martin et al., 2013; Bekker, 2022) and although a short-lived, large-amplitude positive carbon isotope excursion at c. 2.03 Ga has recently been documented in Western Australia (Bekker et al., 2016), the subsequent part of the Paleoproterozoic is characterized by a long-term stability of biogeochemical carbon cycle with seawater dissolved carbon isotope values anchored at ∼0 ‰ with small amplitude (±3–4 ‰) and short-lived variations (Brasier and Lindsay, 1998; Lindsay and Brasier, 2002; Hodgskiss et al., 2019).

The c. 1.98–1.96 Ga Báhkilvárri Formation was deposited on the c. 2.16 Ga Gollebáiki Formation, recording an ∼180-million-year time gap in the stratigraphy of the KGB. This long-lasted hiatus in deposition suggests erosion of the upper part of the *Jatulian* Gollebáiki Formation before the extrusion of basalts and komatiites of the Báhkilvárri Formation. An angular unconformity has been inferred between the Gollebáiki and Báhkilvárri formations even though it is difficult to identify it due to the later Svecofennian deformation (<1.92 Ga) in the area. The orogenic deformation, however, did not produce any yet-recognized major thrusts or detachments between the formations and therefore we consider the boundary between the Gollebáiki and Báhkilvárri formations to be a depositional contact. In contrast, the upper part of the Báhkilvárri Formation is truncated by the Tanaelv Migmatite Belt to the east, and this contact is clearly tectonic (thrust) in the study area.

Very limited, contemporaneous late Ludicovian magmatism is reported from the Central Lapland Greenstone Belt. The Báhkilvárri Formation of the KGB is younger than both the Savukoski and Kittilä groups of the Central Lapland Greenstone Belt, but older than the overlying Kumpu Group (Fig. 12). The Kulkujärvi gabbro hosted in the Kittilä Group has a U-Pb zircon age of 1986 ± 14 Ma (Huhma et al., 2018) corresponds to the late Ludicovian magmatism.

West of the KGB, there are only a few examples of contemporaneous magmatism, e.g., the Dággeborri tonalite pluton in the Kautokeino Greenstone belt (Fig. 12) with a U– Pb zircon age of 1955 ± 7 Ma (Bingen et al., 2015). The intrusion is thus coeval with the intermediate volcanic rocks of the Báhkilvárri Formation in the KGB. A gabbro in the Mjelde-Skorelvvatn Greenstone Belt of the West Troms Basement Complex was dated at 1992 ± 2 Ma (Myhre et al., 2011) and might be coeval with the komatiites in the lower part of the Báhkilvárri Formation.

Late *Ludicovian* gabbroic intrusions also exist farther south and east of the KGB. For example, Hanski (1992, 2014), and Skuf'in and Bayanova (2006) obtained U-Pb and Re-Os ages for the ore-bearing Pilgujärvi gabbro-wehrlite intrusion and co-magmatic ferropicritic volcanics of the Pilgujärvi Volcanic Formation in the Pechenga Belt on the Kola craton in Russia.They report ages of 1988 ± 3 Ma, 1970 ± 5 Ma, and 1987 ± 5 Ma (U-Pb zircon), and 1980 ± 10 Ma (U-Pb baddeleyite). These ages correspond well with ages c. 1.99–1.96 Ga for the Suisari Formation flood basalts and co-magmatic mafic sills and dikes much farther southwest in the Onega province of the Karelia craton (Puchtel et al., 1998; Puchtel et al., 1999; Stepanova et al., 2014; Martin et al., 2015). Interestingly,a similar 1969 ± 1 Ma U-Pb zircon age for tuff in the Kilohigok basin on the Slave craton in NW Canada marks a rift-to-drift transition there (Bowring and Grotzinger, 1992).

These widespread and contemporaneous magmatic events indicate that volcanic rocks of the Báhkilvárri Formation in the KGB correspond to an event that impacted large areas of the Fennoscandian Shield, both on the Karelia and Kola craton, and worldwide. The KGB volcano-sedimentary succession formed during a period of protracted, episodic rifting and continental breakup in northern Fennoscandia, initiated by mantle plume-induced extension and followed by tectonic subsidence and development of shallow-marine basins. This period is also marked in northern Fennoscandia by the emplacement of magmatic intrusions and ultramafic to MORB-type tholeiitic volcanism. The geochronologic and chemostratigraphic constraints presented herein support deposition in an episodically reactivated rift basin under predominantly shallow-marine conditions over the ca. 2.46–1.96 Ga time span with a c. 180-million-year time gap between the early Jatulian Gollebaiki and Ludicovian Bahkilvarri formations.

6.7. Global reconstructions and implications for early Paleoproterozoic evolution

The position of the Karelia-Kola craton within the late Archean supercraton Superia remains uncertain, although most paleogeographical reconstructions place it either along the eastern margin of the Superior craton (Ernst and Bleeker, 2010) or the modern western margin of the Wyoming craton (Davey et al., 2020; Davey et al., 2022). Both reconstructions have the northern to northwestern margin of the Kola-Karelia craton facing the Superia supercraton. Our study highlights protracted, but episodic rifting along this margin of the Kola-Karelia craton between c. 2.5 and 2.0 Ga that eventually led to the development of a passive continental margin. The margin of the neighboring craton to the Karelia-Kola craton in the early Paleoproterozoic should mirror this tectonic evolution. The western and northern margins of the Wyoming craton do not record extension and sedimentary basin development in the early Paleoproterozoic; rather, compressional, metamorphic conditions were documented at c. 2.5–2.45 Ga along these margins (Alcock and Muller, 2012; Cheney et al., 2004; Krogh et al., 2011; Roberts et al., 2002; Mueller et al., 2011, ; see Mammone et al., 2022 for further discussion). In contrast, multiple rifting events were documented along the eastern margin of the Superior craton between c. 2.5 and 2.0 Ga (Ernst and Bleeker, 2010; Hamilton and Buchan, 2016; Milidragovic et al., 2016) and those led to development of sedimentary basins such as the Labrador Trough, and the Mistassini and Otish basins (Clark and Wares, 2005; Chown and Caty, 1973), and, eventually, continental breakup at c. 2.0 Ga (Mammone et al., 2022, and references therein). These basins also contain carbonates that record the LCIE (Melezhik et al., 1997; Bekker et al., 2009). Common tectonic, sedimentary, and geochemical records of the eastern margin of the Superior craton and northern/northwestern margin of the Karelia-Kola cratons in the early Paleoproterozoic thus argue strongly for their shared history and adjacent paleogeographic position.

7. Conclusions

1. New geochronologic and chemostratigraphic data for the volcano-sedimentary succession of the Karasjok Greenstone Belt (KGB) in northwestern Fennoscandia show that its depositional age spans from the Sumian (c. 2.45 Ga) to the upper Ludicovian (c. 1.96 Ga) and that the underlying basement rocks of the Jergul Gneiss Complex are as old as c. 3.0–2.8 Ga. The entire KGB thus records 500 million years of volcanism and sedimentary deposition during a period of protracted, but episodic extension and rifting, and eventual continental breakup of the Superia supercraton, with supracrustal rocks deposited in shallow-water rift basins and in continental passive-margin settings.

2. The oldest Vuomegielas Formation in the northern KGB comprises rhyodacites dated at c. 2.47 Ga, extruded in an intracratonic, extensional (rift) setting likely as a part of the Matachewan mantle plume event on the Karelia, Kola and Superior cratons. The overlying Skuvanvárri Formation is indirectly dated to be of the early Jatulian (>2.2 Ga) age and it contains a thick succession of fuchsite-bearing siliciclastic sedimentary rocks deposited in a subsiding, coastal, deltaic, and shallow-marine basin. The overlying Gollebáiki Formation hosts mid-Jatulian (c. 2.22–2.15 Ga) mafic intrusions and tholeiitic basalts, corresponding to another rifting event on the Fennoscandian Shield that produced large volumes of submarine volcanics in shallow-marine rift basins and continental passive-margin settings. An early Ludicovian (c. 2.06 Ga) age was obtained for the Ni-Cu-PGE-mineralized Porsvann layered intrusion hosted in the Skuvanvárri Formation. The uppermost Báhkilvárre Formation sits unconformably on the Gollebáiki Formation and contains flood basalts, komatiites, and andesitic lavas extruded at c. 1.98–1.96 Ga and represents the final magmatic pulse that covered large area of the Fennoscandian Shield prior to the Lapland–Kola and Svecofennian orogenies.
3. Carbon isotope values for marine carbonates of the Skuvanvárri and Gollebáiki formations are elevated with $\delta^{13}C$ values from + 3.7 to + 12.4 ‰, indicating their deposition during the c. 2.22–2.06 Ga LCIE, when surface environments experienced a rapid rise of atmospheric oxygen and major changes in the global biogeochemical carbon cycle. In contrast, carbonates of the Báhkilvárre Formation have near-to-zero $\delta^{13}C$ values (∼+1.4 ‰), consistent with deposition of this unit in the aftermath of the LCIE.
4. The newly obtained geochronologic and chemostratigraphic data from the Karasjok Greenstone Belt effectively link early Paleoproterozoic evolution of sedimentary basins on the northern Fennoscandian Shield and provide a temporal and stratigraphic framework for further studies into the early Paleoproterozoic evolution of the shield within the Superia supercraton configuration and possible global correlations with other cratons.

Declaration of Competing Interest

The authors declare that they have no known competing financial interests or personal relationships that could have appeared to influence the work reported in this paper.

Data availability

Research data is found as a supplement

Acknowledgments

This work was partly supported by the Research Council of Norway through the funding to The Norwegian Research School on Dynamics and Evolution of Earth and Planets, project number 249040/F60. U-Pb analyses were carried out within the framework of the MiMaC national infrastructure, RCN project number 269842/F50. AB thanks Petroleum Foundation of the American Chemical Society for the grant 624840ND2 that covered stable isotope analyses. Ying Lin helped with C and O isotope analyses at UCR. We would like to thank A. Peterson and M. Satish-Kumar for their helpful comments and V. Pease for editorial handling.

Appendix A. Supplementary data

Supplementary data to this article can be found online at https://doi.org/10.1016/j.precamres.2023.107166.

References

Ahtonen, N., Hölttä, P., Huhma, H., 2007. Intracratonic Palaeoproterozoic granitoids in northern Finland: prolonged and episodic crustal melting events revealed by Nd isotopes and U-Pb ages on zircon. Bull. Geol. Soc. Finland 79, 143–174. https://doi.org/10.17741/bgsf/79.2.002.

Alcock, J., Muller, P., 2012. A Paleoproterozoic sedimentary basin within the Wyoming cratonexposed in the Ruby Range. SW Montana: Identified by fieldrelations and geochronology. Northwest Geology, pp. 47–62.

Alfimova, N.A., Kuznetsov, A.B., V.Klimova, E., Bekker, A., 2022. Archean-Proterozoic unconformity on the Fennoscandian Shield: Geochemistry and Sr, C and O isotope composition of Paleoproterozoic carbonate-rich regolith from Segozero Lake (Russian Karelia). Precambr. Res. 368, 106459. https://doi.org/10.1016/j.precamres.2021.106459.

Amelin, Y., Heaman, L., Semenov, V., 1995. U-Pb geochronology of layered mafic intrusions in the eastern Baltic Shield: implications for the timing and duration of Paleoproterozoic continental rifting. Precambr. Res. 75, 31–46. https://doi.org/10.1016/0301-9268(95)00015-W.

Andreassen, T.O., 1993. Strukturelle og tektoniske undersøkelser i de nordlige deler av Karasjok grønnsteinsbelte, Finnmark fylke. Cand. scient. thesis. University of Tromsø, p. 148 (in Norwegian).

Baker, A., Fallick, A., 1989a. Heavy carbon in two-billion-year-old marbles fromLofoten-Vesterålen, Norway: Implications for the Precambrian carbon cycle. Geochim. Cosmochim. Acta 53, 1111–1115. https://doi.org/10.1016/0016-7037(89)90216-0.

Baker, A.J., Fallick, A.E., 1989b. Evidence from Lewisian limestones for isotopically heavy carbon in two-thousand-million-year-old sea water. Nature 337, 352–354. https://doi.org/10.1038/337352a0.

Barnes, S.J., Often, M., 1990. Ti-rich komatiites from northern Norway. Contrib. Miner. Petrol. 105, 42–54. https://doi.org/10.1007/BF00320965.

Baumgartner, L.P., Valley, J.W., 2001. Stable isotope transport and contact metamorphic fluid flow. Rev. Mineral. Geochem. 43, 415–467. https://doi.org/10.2138/gsrmg.43.1.415.

Bayanova, T., Korchagin, A., Mitrofanov, A., Serov, P., Ekimova, N., Nitkina, E., Kamensky, I., Elizarov, D., Huber, M., 2019. Long-lived mantle plume and polyphase evolution of Palaeoproterozoic PGE intrusions in the Fennoscandian Shield. Minerals 9, 59. https://doi.org/10.3390/min9010059.

Bayanova, T., Ludden, J., Mitrofanov, F., 2009. Timing and duration of Palaeoproterozoic events producing ore-bearing layered intrusions of the Baltic Shield: metallogenic, petrological and geodynamic implications, in: Reddy, S.M., Mazumder, R., Evans, D.A.D., Collins, A.S. (Eds.), Palaeoproterozoic Supercontinents and Global Evolution. Geological Society of London. volume 323 of Special Publications, pp. 165–198. doi:10.1144/sp323.8.

Bekker, A., 2022. Lomagundi carbon isotope excursion. In: Encyclopedia of Astrobiology. Springer, Berlin Heidelberg, pp. 1–7. https://doi.org/10.1007/978-3-642-27833-4_5127-2.

Bekker, A., Davis, D., Wing, B., 2009. Chemostratigraphy and geochronology of the Kaniapiskau Supergroup, Labrador Trough indicate a major tectonic reorganization event hidden in the first cycle. Program with Abstracts. Abstract ID U21D–09.

Bekker, A., Eriksson, K.A., 2003. A Paleoproterozoic drowned carbonate platform on the southeastern margin of the Wyoming Craton: a record of the Kenorland breakup. Precambr. Res. 120, 327–364. https://doi.org/10.1016/s0301-9268(02)00165-1.

Bekker, A., Holland, H., 2012. Oxygen overshoot and recovery during the early Paleoproterozoic. Earth Planet. Sci. Lett. 317–318, 295–304. https://doi.org/10.1016/j.epsl.2011.12.012.

Bekker, A., Karhu, J., Eriksson, K., Kaufman, A., 2003. Chemostratigraphy of Paleoproterozoic carbonate successions of the Wyoming Craton: tectonic forcing of biogeochemical change? Precambr. Res. 120, 279–325. https://doi.org/10.1016/s0301-9268(02)00164-x.

Bekker, A., Karhu, J., Kaufman, A., 2006. Carbon isotope record for the onset of the Lomagundi carbon isotope excursion in the Great Lakes area, North America. Precambr. Res. 148, 145–180. https://doi.org/10.1016/j.precamres.2006.03.008.

Bekker, A., Kaufman, A., Karhu, J., Eriksson, K., 2005. Evidence for Paleoproterozoic cap carbonates in North America. Precambr. Res. 137, 167–206. https://doi.org/10.1016/j.precamres.2005.03.009.

Bekker, A., Krapež, B., Müller, S.G., Karhu, J.A., 2016. A short-term, post-Lomagundi positive C isotope excursion at c. 2.03 Ga recorded by the Wooly Dolomite, Western Australia. J. Geol. Soc. 173, 689–700. https://doi.org/10.1144/jgs2015-152.

Bergh, S.G., Kullerud, K., Armitage, P.E., Zwaan, K.B., Corfu, F., Ravna, E.J., Myhre, P.I., 2010. Neoarchaean to Svecofennian tectono-magmatic evolution of the West Troms Basement Complex, North Norway. Norw. J. Geol. 90, 21–48.

Bergh, S.G., Kullerud, K., Corfu, F., Armitage, P.E., Davidsen, B., Johansen, H.W., Pettersen, T., Knudsen, S., 2007. Low-grade sedimentary rocks on Vanna, North Norway: a new occurrence of a Palaeoproterozoic (2.4-2.2 Ga) cover succession in northern Fennoscandia. Norw. J. Geol. 87, 301–318.

Bergh, S.G., Kullerud, K., Myhre, P.I., Corfu, F., Armitage, P.E.B., Zwaan, K.B., Ravna, E. J.K., 2014. Archaean elements of the basement outliers west of the Scandinavian Caledonides in Northern Norway: Architecture, evolution and possible correlation with Fennoscandia, in: Dilek, Y., Furnes, H. (Eds.), Evolution of Archean Crust and Early Life. Springer Netherlands, Dordrecht. volume 7 of Modern Approaches in Solid Earth Sciences. chapter 4, pp. 103–126. doi:10.1007/978-94-007-7615-9_4.

Bergh, S.G., Torske, T., 1986. The Proterozoic Skoadduvarri Sandstone Formation, Alta, Northern Norway: A tectonic fan-delta complex. Sed. Geol. 47, 1–25. https://doi.org/10.1016/0037-0738(86)90068-0.

Bergh, S.G., Torske, T., 1988. Palaeovolcanology and tectonic setting of a Proterozoic metatholeiitic sequence near the Baltic Shield margin, northern Norway. Precambr. Res. 39, 227–246. https://doi.org/10.1016/0301-9268(88)90021-6.

Bingen, B., Solli, A., Viola, G., Torgersen, E., Sandstad, J.S., Whitehouse, M.J., Røhr, T.S., Ganerød, M., Nasuti, A., 2015. Geochronology of the Palaeoproterozoic Kautokeino Greenstone Belt, Finnmark, Norway: Tectonic implications in a Fennoscandia context. Norw. J. Geol. 95, 365–396. https://doi.org/10.17850/njg95-3-09.

Bjerkgård, T., Slagstad, T., Henderson, I.H., Sandstad, J.S., Schönenberger, J., 2015. Geology and gold mineralisation in the Mauken Precambrian basement window, Målselv, Troms, northern Norway. Norw. J. Geol. 95, 423–443. https://doi.org/10.17850/njg95-3-08.

Bleeker, W., 2003. The late Archean record: a puzzle in ca. 35 pieces. Lithos 71, 99–134. https://doi.org/10.1016/j.lithos.2003.07.003.

Bowring, S.A., Grotzinger, J.P., 1992. Implications of new chronostratigraphy for tectonic evolution of Wopmay Orogen, Northwest Canadian Shield. Am. J. Sci. 292, 1–20. https://doi.org/10.2475/ajs.292.1.1.

Braathen, A., 1993. Stratigrafi og strukturgeologi sentralt i Karasjok grønnsteinsbelte, Finnmark. Cand. scient thesis. University of Tromsø. 130 pp. (In Norwegian).

Braathen, A., Davidsen, B., 2000. Structure and stratigraphy of the Palaeoproterozoic Karasjok Greenstone Belt, north Norway - regional implications. Nor. Geol. Tidsskr. 80, 33–50.

Brasier, M.D., Lindsay, J.F., 1998. A billion years of environmental stability and the emergence of eukaryotes: New data from northern Australia. Geology 26, 555–558.

Chashchin, V.V., Bayanova, T.B., Levkovich, N.V., 2008. Volcanoplutonic association of the early-stage evolution of the Imandra-Varzuga rift zone, Kola Peninsula, Russia: Geological, petrogeochemical, and isotope-geochronological data. Petrology 16, 279–298. https://doi.org/10.1134/s0869591108030041.

Cheney, J.T., Brady, J.B., Tierney, K.A., DeGraff, K.A., Mohlman, H.K., Frisch, J.D., Hatch, C.E., Steiner, M.L., Carmichael, S.K., Fisher, R.G., Tuit, C.B., J. Steffen, K., Cady, P., Lowell, J., Archuleta, L.L., Hirst, J., Wegmann, K.W., BrianMonteleone, 2004. Proterozoic Metamorphism of the Tobacco Root Mountains, Montana, in: Brady, J., Burger, H., Cheney, J., Harms, T. (Eds.), Precambrian Geology of the Tobacco Root Mountains. number 377 in Geological Society of America Special Paper, pp. 105–129. URL: https://scholarworks.smith.edu/geo_facpubs/33.

Chown, E., Caty, J., 1973. Stratigraphy, petrography and paleocurrent analysis of the Aphebian clastic formations of the Mistassini-Otish Basin. Geol. Assoc. Can. Spec. Pap. 12, 49–71.

Ciborowski, T.J.R., Kerr, A.C., Ernst, R.E., McDonald, I., Minifie, M.J., Harlan, S.S., Millar, I.L., 2015. The Early Proterozoic Matachewan Large Igneous Province: Geochemistry, petrogenesis, and implications for Earth evolution. J. Petrol. 56, 1459–1494. https://doi.org/10.1093/petrology/egv038.

Clark, T., Wares, R., 2005. Lithotectonic and metallogenic synthesis of the New Québec Orogen (Labrador Trough). MM2005-01, 175 pp.

Corfu, F., 2007. Multistage metamorphic evolution and nature of the amphibolite–granulite facies transition in Lofoten-Vesterålen, Norway, revealed by U-Pb in accessory minerals. Chem. Geol. 241, 108–128. https://doi.org/10.1016/j.chemgeo.2007.01.028.

Daly, J.S., Balagansky, V.V., Timmerman, M.J., Whitehouse, M.J., 2006. The Lapland-Kola orogen: Palaeoproterozoic collision and accretion of the northern Fennoscandianlithosphere, in: Gee, D.G., Stephenson, R.A. (Eds.), European Lithosphere Dynamics. Geological Society of London. volume 32 of Memoirs, pp. 579–598. doi:10.1144/gsl.mem.2006.032.01.35.

Davey, S., Bleeker, W., Kamo, S., Vuollo, J., Ernst, R., Cousens, B., 2020. Archean block rotation in Western Karelia: Resolving dyke swarm patterns in metacraton Karelia-Kola for a refined paleogeographic reconstruction of supercraton Superia. Lithos 368–369, 105553. https://doi.org/10.1016/j.lithos.2020.105553.

Davey, S.C., Bleeker, W., Kamo, S.L., Ernst, R.E., Cousens, B.L., Vuollo, J., Huhma, H., 2022. Evidence for a Single Large Igneous Province at 2.11 Ga across Supercraton Superia. J. Petrol. 63. https://doi.org/10.1093/petrology/egac038.

Davidsen, B., 1994. Stratigrafi, petrologi og geokjemi med vekt på komatiittiske bergarter innen den nordligste del av Karasjok grønnsteinsbelte. Cand. scient. thesis. University of Tromsø.

Elvebakk, G., Krill, A.G., Often, M., Henriksen, H., 1985. Early proterozoic shallow-marine albite-rich sandstone in the Karasjok Greenstone Belt, Norway. Norges Geologiske Undersøkelse Bulletin 403, 113–118. URL: https://hdl.handle.net/11250/2674248.

Ernst, R., Bleeker, W., 2010. Large igneous provinces (LIPs), giant dyke swarms, and mantle plumes: significance for breakup events within Canada and adjacent regions from 2.5 Ga to the Present. Can. J. Earth Sci. 47, 695–739. https://doi.org/10.1139/e10-025.

Gaál, G., Gorbatschev, R., 1987. An outline of the precambrian evolution of the baltic shield. Precambr. Res. 35, 15–52. https://doi.org/10.1016/0301-9268(87)90044-1.

Griffin, W.L., Taylor, P.N., Hakkinen, J.W., Heier, K.S., Iden, I.K., Krogh, E.J., Malm, O., Olsen, K.I., Ormaasen, D.E., Tveten, E., 1978. Archaean and Proterozoic crustal evolution in Lofoten-Vesterålen, N Norway. J. Geol. Soc. 135, 629–647. https://doi.org/10.1144/gsjgs.135.6.0629.

Gumsley, A.P., Chamberlain, K.R., Bleeker, W., Söderlund, U., de Kock, M.O., Larsson, E. R., Bekker, A., 2017. Timing and tempo of the Great Oxidation Event. Proc. Nat. Acad. Sci. 114, 1811–1816. https://doi.org/10.1073/pnas.1608824114.

Hamilton, M.A., Buchan, K.L., 2016. A 2169 Ma U-Pb baddeleyite age for the Otish Gabbro, Quebec: implications for correlation of Proterozoic magmatic events and sedimentary sequences in the eastern Superior Province. Can. J. Earth Sci. 53, 119–128. https://doi.org/10.1139/cjes-2015-0131.

Hansen, H., 2008. Tectonic setting, magmatic evolution and PGE-potentiality of the layered intrusions in Karasjok Greenstone Belt, Finnmark, northern Norway. Master's thesis. University of TromsøFaculty of Science, Department of geology.

Hanski, E., 1992. Petrology of the Pechenga ferropicrites and cogenetic, Ni-bearing gabbro-wehrlite intrusions, Kola Peninsula, Russia. Geological Survey og Finland, Bulletin 367, 1–192. URL: http://tupa.gtk.fi/julkaisu/bulletin/bt_367.pdf. dissertation: University of Oulu, Faculty of science.

Hanski, E., Huhma, H., 2005. Central Lapland Greenstone Belt, in: Lehtinen, M., Nurmi, P., Rämö, O. (Eds.), Precambrian Geology of Finland — Key to the Evolution of the Fennoscandian Shield. Elsevier. volume 14 of Developments in Precambrian Geology. chapter 4, pp. 139–193. doi: 10.1016/S0166-2635(05)80005-2.

Hanski, E., Huhma, H., Rastas, P., Kamenetsky, V.S., 2001. The Palaeoproterozoic Komatiite-Picrite Association of Finnish Lapland. J. Petrol. 42, 855–876. https://doi.org/10.1093/petrology/42.5.855.

Hanski, E., Huhma, H., Vuollo, J., 2010. SIMS zircon ages and Nd isotope systematics of the 2.2 Ga mafic intrusions in northern and eastern Finland. In: Bulletin of the Geological Society of Finland URL.

Hanski, E.J., 2013. Evolution of the Palaeoproterozoic (2.50–1.95 Ga) non-orogenic magmatism in the eastern part of the Fennoscandian Shield, in: Melezhik, V.A., Prave, A.R., Hanski, E.J., Fallick, A.E., Lepland, A., Kump, L.R., Strauss, H. (Eds.), Reading the Archive of Earth's Oxygenation. Springer, Berlin Heidelberg. Frontiers in Earth Sciences. chapter 3.4, pp. 179–245. doi:10.1007/978-3-642-29682-6_6.

Hanski, E.J., Huhma, H., Melezhik, V.A., 2014. New isotopic and geochemical data from the Palaeoproterozoic Pechenga Greenstone Belt, NW Russia: Implication for basin development and duration of the volcanism. Precambr. Res. 245, 51–65. https://doi.org/10.1016/j.precamres.2014.01.008.

Hanski, E.J., Melezhik, V.A., 2013. Litho- and chronostratigraphy of the Palaeoproterozoic Karelian formations, in: Melezhik, V.A., Prave, A.R., Hanski, E.J., Fallick, A.E., Lepland, A., Kump, L.R., Strauss, H. (Eds.), Reading the Archive of Earth's Oxygenation. Springer, Berlin Heidelberg. Frontiers in Earth Sciences. chapter 3.2, pp. 39–110. doi:10.1007/978-3-642-29682-6_4.

Haverinen, J., 2020. Evaporites in the Central Lapland Greenstone Belt. Master's thesis. University of Helsinki, Department of Geosciences and Geology. URL: http://urn.fi/URN:NBN:fi:hulib-202101081117.

Heaman, L.M., 1997. Global mafic magmatism at 2.45 Ga: Remnants of an ancient large igneous province? Geology 25, 299. https://doi.org/10.1130/0091-7613(1997)025<0299:gmmagr>2.3.co;2.

Henderson, I.H., Viola, G., Nasuti, A., 2015. A new tectonic model for the Palaeoproterozoic Kautokeino Greenstone Belt, northern Norway, based on high-resolution airborne magnetic data and field structural analysis and implications for mineral potential. Norw. J. Geol. 95, 339–364. https://doi.org/10.17850/njg95-3-05.

Hodgskiss, M.S., Dagnaud, O.M., Frost, J.L., Halverson, G.P., Schmitz, M.D., Swanson-Hysell, N.L., Sperling, E.A., 2019. New insights on the Orosirian carbon cycle, early Cyanobacteria, and the assembly of Laurentia from the Paleoproterozoic Belcher Group. Earth Planet. Sci. Lett. 520, 141–152. https://doi.org/10.1016/j.epsl.2019.05.023.

Huhma, H., Hanski, E., Kontinen, A., Vuollo, J., Mänttäri, I., Lahaye, Y., 2018. Sm–Nd and U–Pb isotope geochemistry of the Palaeoproterozoic mafic magmatism in eastern and northern Finland. Bulletin 405. Geological Survey of Finland. Espoo. URL: http://tupa.gtk.fi/julkaisu/bulletin/bt_405.pdf. 150 pages, 128 figures, 1 table and 11 appendices.

Iljina, M., Hanski, E., 2005. Layered mafic intrusions of the Tornio-Näränkävaara belt, in: Lehtinen, M., Nurmi, P., Rämö, O. (Eds.), Precambrian Geology of Finland — Key to the Evolution of the Fennoscandian Shield. Elsevier. volume 14 of Developments in Precambrian Geology. chapter 3, pp. 101–137. doi:10.1016/s0166-2635(05)80004-0.

Iljina, M., Maier, W., Karinen, T., 2015. PGE-(Cu-Ni) deposits of the Tornio-Näränkävaara Belt of intrusions (Portimo, Penikat, and Koillismaa). In: Maier, W.D., Lahtinen, R., O'Brien, H. (Eds.), Mineral Deposits of Finland, chapter 3.3. Elsevier, Amsterdam, pp. 133–164. https://doi.org/10.1016/b978-0-12-410438-9.00005-4.

Jackson, S.E., Pearson, N.J., Griffin, W.L., Belousova, E.A., 2004. The application of laser ablation-inductively coupled plasma-mass spectrometry to in situ U-Pb zircon geochronology. Chem. Geol. 211, 47–69. https://doi.org/10.1016/j.chemgeo.2004.06.017.

Johannesen, H., 2012. Tinnvatnformasjonen i Vannas proterozoiske lagrekke: Sedimentære facies og avsetningsmiljø. Master's thesis. Department of geosciences, University of Tromsø. URL: https://hdl.handle.net/10037/4319. (In Norwegian).

Järvinen, V., Halkoaho, T., Konnunaho, J., Heinonen, J.S., Rämö, O.T., 2019. Parental magma, magmatic stratigraphy, and reef-type PGE enrichment of the 2.44 Ga mafic-ultramafic Näränkävaara layered intrusion. Northern Finland. Mineralium Deposita 55, 1535–1560. https://doi.org/10.1007/s00126-019-00934-z.

Karhu, J.A., 1993. Paleoproterozoic evolution of the carbon isotope ratios of sedimentary carbonates in the Fennoscandian Shield. Geological Survey of Finland Bulletin 371, 1–87. URL: http://tupa.gtk.fi/julkaisu/bulletin/bt_371.pdf.

Karhu, J.A., Holland, H.D., 1996. Carbon isotopes and the rise of atmospheric oxygen. Geology 24, 867. https://doi.org/10.1130/0091-7613(1996)024<0867:ciatro>2.3.co;2.

Kilian, T.M., Bleeker, W., Chamberlain, K., Evans, D.A.D., Cousens, B., 2015. Palaeomagnetism, geochronology and geochemistry of the Palaeoproterozoic Rabbit Creek and Powder River dyke swarms: implications for Wyoming in supercraton Superia. Geological Society, London, Special Publications 424, 15–45. https://doi.org/10.1144/sp424.7.

Kilian, T.M., Chamberlain, K.R., Evans, D.A., Bleeker, W., Cousens, B.L., 2016. Wyoming on the run—Toward final Paleoproterozoic assembly of Laurentia. Geology 44, 863–866. https://doi.org/10.1130/g38042.1.

Krill, A., Bergh, S.G., Lindahl, I., Mearns, E., Often, M., Olerud, S., Olesen, O., Sandstad, J.S., Siedlecka, A., Solli, A., 1985. Rb-Sr, U-Pb and Sm-Nd isotopic dates from Precambrian rocks of Finnmark. Norges Geologiske Undersøkelse Bulletin 403, 37–54. URL: https://hdl.handle.net/11250/2674245.

Krill, A.G., 1985. Svekokarelian thrusting with thermal inversion in the Karasjok-Levajok area of the northern Baltic Shield. Norges Geologiske Undersøkelse Bulletin 403, 89–101. URL: https://hdl.handle.net/11250/2674242.

Krogh, T.E., Kamo, S.L., Hanley, T.B., Hess, D.F., Dahl, P.S., Johnson, R.E., 2011. Geochronology and geochemistry of Precambrian gneisses, metabasites, and pegmatite from the Tobacco Root Mountains, northwestern Wyoming craton, Montana. Can. J. Earth Sci. 48, 161–185. https://doi.org/10.1139/e10-095.

Kulikov, V.S., Bychkova, Y.V., Kulikova, V.V., Ernst, R., 2010. The Vetreny Poyas (Windy Belt) subprovince of southeastern Fennoscandia: An essential component of the ca. 2.5–2.4 Ga Sumian large igneous provinces. Precambr. Res. 183, 589–601. https://doi.org/10.1016/j.precamres.2010.07.011.

Kulikov, V.S., Bychkova, Y.V., Kulikova, V.V., Kostitsyn, Y.A., Pokrovsky, O.S., Vasil'ev, M.V., 2008. The Ruiga intrusion: A typical example of a shallow-facies paleoproterozoic peridotite-gabbro-komatiite-basaltic association of the Vetreny Belt, southeastern Fennoscandia. Petrology 16, 531–551. https://doi.org/10.1134/s0869591108060015.

Köykkä, J., Lahtinen, R., Huhma, H., 2019. Provenance evolution of the Paleoproterozoic metasedimentary cover sequences in northern Fennoscandia: Age distribution, geochemistry, and zircon morphology. Precambr. Res. 331, 105364. https://doi.org/10.1016/j.precamres.2019.105364.

Köykkä, J., Lahtinen, R., Manninen, T., 2022. Tectonic evolution, volcanic features and geochemistry of the Paleoproterozoic Salla belt, northern Fennoscandia: From 2.52 to 2.40 Ga LIP stages to ca. 1.92–1.90 Ga collision. Precambr. Res. 371, 106597. https://doi.org/10.1016/j.precamres.2022.106597.

Lahtinen, R., Garde, A.A., Melezhik, V.A., 2008. Paleoproterozoic evolution of Fennoscandia and Greenland. Episodes 31, 20–28.

Lahtinen, R., Huhma, H., 2019. A revised geodynamic model for the Lapland-Kola Orogen. Precambr. Res. 330, 1–19. https://doi.org/10.1016/j.precamres.2019.04.022.

Lahtinen, R., Korja, A., Nironen, M., 2005. Paleoproterozoic tectonic evolution, in: Lehtinen, M., Nurmi, P., Rämö, O. (Eds.), Precambrian Geology of Finland — Key to the Evolution of the Fennoscandian Shield. Elsevier. volume 14 of Developments in Precambrian Geology. chapter 11, pp. 481–531. doi:10.1016/s0166-2635(05)80012-x.

Lahtinen, R., Köykkä, J., 2020. Multiply deformed Paleoproterozoic foreland fold and thrust belt in northern Fennoscandia – The peripheral Kuusamo belt as a key example. Precambr. Res. 346, 105825. https://doi.org/10.1016/j.precamres.2020.105825.

Laurent, O., Auwera, J.V., Bingen, B., Bolle, O., Gerdes, A., 2019. Building up the first continents: Mesoarchean to Paleoproterozoic crustal evolution in West Troms, Norway, inferred from granitoid petrology, geochemistry and zircon U-Pb/Lu-Hf isotopes. Precambr. Res. 321, 303–327. https://doi.org/10.1016/j.precamres.2018.12.020.

Lauri, L.S., Andersen, T., Hölttä, P., Huhma, H., Graham, S., 2011. Evolution of the Archaean Karelian Province in the Fennoscandian Shield in the light of U-Pb zircon ages and Sm–Nd and Lu–Hf isotope systematics. J. Geol. Soc. 168, 201–218. https://doi.org/10.1144/0016-76492009-159.

Lauri, L.S., Mikkola, P., Karinen, T., 2012. Early paleoproterozoic felsic and mafic magmatism in the Karelian province of the Fennoscandian shield. Lithos 151, 74–82. https://doi.org/10.1016/j.lithos.2012.01.013.

Lauri, L.S., Mänttäri, I., 2002. The Kynsijärvi quartz alkali feldspar syenite, Koillismaa, eastern Finland—silicic magmatism associated with 2.44 Ga continental rifting. Precambr. Res. 119, 121–140. https://doi.org/10.1016/s0301-9268(02)00120-1.

Li, Y., Satish-Kumar, M., Kiran, S., Wan, C., Zheng, J., 2022. 2.0 Ga orogenic graphite deposits and associated 13c-enriched meta-carbonate rocks from South China Craton: Implications for global Lomagundi event. Geosci. Front. 13, 101409. https://doi.org/10.1016/j.gsf.2022.101409.

Lindsay, J.F., Brasier, M.D., 2002. Did global tectonics drive early biosphere evolution? Carbon isotope record from 2.6 to 1.9 Ga carbonates of Western Australian basins. Precambr. Res. 114, 1–34. https://doi.org/10.1016/s0301-9268(01)00219-4.

Ludwig, K.R., 2008. User's manual for Isoplot 3.70 - A Geochronological Toolkit for Microsoft Excel. Berkeley Geochronology Center. URL: https://www.bgc.org/isoplot.

Maier, W.D., Halkoaho, T., Huhma, H., Hanski, E., Barnes, S.J., 2018. The Penikat intrusion, Finland: Geochemistry, geochronology, and origin of Platinum-Palladium reefs. J. Petrol. 59, 967–1006. https://doi.org/10.1093/petrology/egy051.

Mammone, N., Bekker, A., Chamberlain, K., Kuznetsov, A., 2022. Testing the early Paleoproterozoic connection of the Superior and Wyoming cratons with geochronology and geochemistry. Precambr. Res. 381, 106818. https://doi.org/10.1016/j.precamres.2022.106818.

Manninen, T., Pihlaja, P., Huhma, H., 2001. U-Pb geochronology of the Peurasuvanto area, northern Finland, in: Vaasjoki, M. (Ed.), Radiometric age determinations from Finnish Lapland and their bearing on the timing of Precambrian volcano-sedimentary sequences. Geological Survey of Finland. volume 33 of Special Paper, pp. 189–200. URL: http://tupa.gtk.fi/julkaisu/specialpaper/sp_033.pdf. 5 figures, one table and one appendix.

Martin, A., Condon, D., Prave, A., Melezhik, V., Lepland, A., Fallick, A., 2013. Dating the termination of the Palaeoproterozoic Lomagundi-Jatuli carbon isotopic event in the North Transfennoscandian Greenstone Belt. Precambr. Res. 224, 160–168. https://doi.org/10.1016/j.precamres.2012.09.010.

Martin, A., Prave, A., Condon, D., Lepland, A., Fallick, A., Romashkin, A., Medvedev, P., Rychanchik, D., 2015. Multiple Palaeoproterozoic carbon burial episodes and excursions. https://doi.org/10.1016/j.epsl.2015.05.023.

Martin, A.P., Condon, D.J., Prave, A.R., Lepland, A., 2013. A review of temporal constraints for the Palaeoproterozoic large, positive carbonate carbon isotope excursion (the Lomagundi-Jatuli Event). Earth Sci. Rev. 127, 242–261. https://doi.org/10.1016/j.earscirev.2013.10.006.

Master, S., Bekker, A., Karhu, J.A., 2013. Paleoproterozoic high $\delta^{13}C_{carb}$ marbles from the Ruwenzori Mountains, Uganda: Implications for the age of the Buganda Group. Chem. Geol. 362, 157–164. https://doi.org/10.1016/j.chemgeo.2013.10.005.

Melezhik, V.A., Bingen, B., Sandstad, J.S., Pokrovsky, B.G., Solli, A., Fallick, A.E., 2015. Sedimentary-volcanic successions of the Alta-Kvænangen Tectonic Window in the northern Norwegian Caledonides: Multiple constraints on deposition and correlation with complexes on the Fennoscandian Shield. Norw. J. Geol. 95, 245–284. https://doi.org/10.17850/njg95-3-01.

Melezhik, V.A., Fallick, A.E., Clark, T., 1997. Two billion year old isotopically heavy carbon: evidence from the Labrador Trough. Canada. https://doi.org/10.1139/e17-025.

Melezhik, V.A., Hanski, E.J., 2013a. The early palaeoproterozoic of fennoscandia: Geological and tectonic settings, in: Melezhik, V.A., Prave, A.R., Hanski, E.J., Fallick, A.E., Lepland, A., Kump, L.R., Strauss, H. (Eds.), Reading the Archive of Earth's Oxygenation. Springer. Volume 1: The Palaeoproterozoic of Fennoscandia as Context for the Fennoscandian Arctic Russia - Drilling Early Earth Project. chapter 3.1, pp. 33–38. doi:10.1007/978-3-642-29682-6_3.

Melezhik, V.A., Hanski, E.J., 2013b. Palaeotectonic and Palaeogeographic Evolution of Fennoscandia in the Early Palaeoproterozoic, in: Melezhik, V.A., Prave, A.R., Hanski, E.J., Fallick, A.E., Lepland, A., Kump, L.R., Strauss, H. (Eds.), Reading the Archive of Earth's Oxygenation. Springer. Frontiers in Earth Sciences. chapter 3.3, pp. 111–178. doi:10.1007/978-3-642-29682-6_5.

Melezhik, V.A., Huhma, H., Condon, D.J., Fallick, A.E., Whitehouse, M.J., 2007. Temporal constraints on the Paleoproterozoic Lomagundi-Jatuli carbon isotopic event. Geology 35, 655. https://doi.org/10.1130/g23764a.1.

Melezhik, V.A., Solli, A., Fallick, A.E., Davidsen, B., 2015. Chemostratigraphic constraints on the time of deposition of carbonate rocks in the Karasjok Greenstone Belt, northern Norway. Norw. J. Geol. 95, 299–314. https://doi.org/10.17850/njg95-3-03.

Melezhik, V.A., Young, G.M., Eriksson, P.G., Altermann, W., Kump, L.R., Lepland, A., 2013. Huronian-age glaciation, in: Melezhik, V.A., Prave, A.R., Hanski, E.J., Fallick, A.E., Lepland, A., Kump, L.R., Strauss, H. (Eds.), Reading the Archive of Earth's Oxygenation. Springer, Berlin Heidelberg. Frontiers in Earth Sciences. chapter 7.2, pp. 1059–1109. doi:10.1007/978-3-642-29670-3_2.

Milidragovic, D., Beaudoin, G., Hamilton, M.A., King, J.J., 2016. The Paleoproterozoic Otish Gabbro suite and coeval dyke swarms of the Superior Province: Probing the ca. 2.17 Ga mantle. Precambr. Res. 278, 126–144. https://doi.org/10.1016/j.precamres.2016.03.012.

Moilanen, M., Hanski, E., Yang, S.H., 2021. Re-Os isotope geochemistry of the Palaeoproterozoic Sakatti Cu-Ni-PGE sulphide deposit in northern Finland. Ore Geol. Rev. 132, 104044. https://doi.org/10.1016/j.oregeorev.2021.104044.

Mueller, P., Wooden, J., Mogk, D., 2011. 2450 Ma Metamorphism recorded in 3250 Ma Geisses, Gallatin Range. Montana. Northwest Geology 1–8.

Mun, Y., Palinkas, S.S., Kullerud, K., Nilsen, K.S., Neufeld, K., Bekker, A., 2020. Evolution of metal-bearing fluids at the Nussir and Ulveryggen sediment-hosted Cu deposits, Repparfjord Tectonic Window, northern norway. Norw. J. Geol. https://doi.org/10.17850/njg100-2-5.

Murakami, T., Chakoumakos, B.C., Ewing, R.C., Lumpkin, G.R., Weber, W.J., 1991. Alpha-decay event damage in zircon. Am. Mineral. 76, 1510–1532.

Mutanen, T., Huhma, H., 2001. U-Pb geochronology of the Koitelainen, Akanvaara and Keivitsa layered intrusions and related rocks, in: Vaasjoki, M. (Ed.), Radiometric age determinations from Finnish Lapland and their bearing on the timing of Precambrian volcano-sedimentary sequences. Geological Survey of Finland. volume 33 of Special Paper, pp. 229–246. URL: http://tupa.gtk.fi/julkaisu/specialpaper/sp_033.pdf. 13 figures, one table and one appendix.

Mutanen, T., Huhma, H., 2003. The 3.5 Ga Siurua trondhjemite gneiss in the Archaean Pudasjärvi Granulite Belt, northern Finland. Bulletin of the Geological Society of Finland 75, 51–68. https://doi.org/10.17741/bgsf/75.1-2.004.

Myhre, P.I., Corfu, F., Bergh, S.G., 2011. Palaeoproterozoic (2.0–1.95 Ga) pre-orogenic supracrustal sequences in the West Troms Basement Complex. North Norway. Precambrian Research 186, 89–100. https://doi.org/10.1016/j.precamres.2011.01.003.

Myhre, P.I., Corfu, F., Bergh, S.G., Kullerud, K., 2013. U-Pb geochronology along an Archaean geotransect in the West Troms Basement Complex, North Norway. Norw. J. Geol. 93, 1–24. URL: https://njg.geologi.no/vol-91-100/details/1/24-24.html.

Myskova, T.A., Ivanov, N.M., Korsakova, M.A., Mil'kevich, R.I., Berezhnaya, N.G., Presnyakov, S.L., 2013. Geology, geochemistry, and age of volcanites of the Tunguda Volcanic Formation: The problem of the Archean-Proterozoic boundary in North Karelia. Stratigr. Geol. Correl. 21, 337–358. https://doi.org/10.1134/s0869593813040072.

Nasuti, A., Roberts, D., Dumais, M.A., Ofstad, F., Hyvönen, E., Stampolidis, A., Rodionov, A., 2015. New high-resolution aeromagnetic and radiometric surveys in Finnmark and North Troms: linking anomaly patterns to bedrock geology and structure. Norw. J. Geol. 95, 217–244. https://doi.org/10.17850/njg95-3-10.

Nilsen, K.S., 1998. Bergrunnsgeologisk kart Hal'kavarri 2034 I, M 1:50 000, revidert foreløpig utgave. Norges Geologiske Undersøkelse.

Nilsson, L.P., Often, M., 2005. A summary report on the Ni-Cu-PGE occurrences and their host rocks in the Precambrian of Finnmark. Geological Survey of Norway, Northern Norway. NGU report 2005.085.

Often, M., 1985. The Early Proterozoic Karasjok Greenstone Belt, Norway: a preliminary description of lithology, stratigraphy and mineralization. Norges Geologiske Undersøkelse Bulletin 403, 75–88. URL: https://hdl.handle.net/11250/2674246.

Ojakangas, R.W., Marmo, J.S., Heiskanen, K.I., 2001. Basin evolution of the Paleoproterozoic Karelian Supergroup of the Fennoscandian (Baltic) Shield. Sed. Geol. 141–142, 255–285. https://doi.org/10.1016/s0037-0738(01)00079-3.

Olesen, O., Sandstad, J.S., 1993. Interpretation of the Proterozoic Kautokeino Greenstone Belt, Finnmark, Norway from combined geophysical and geological data. Norges Geologiske Undersøkelse Bulletin 425, 43–62. URL: http://www.ngu.no/FileArchive/NGUPublikasjoner/Bulletin425_43-62.pdf.

Orvik, A.A., Slagstad, T., Hansen, H., Nilsson, L.P., Sørensen, B.E., 2022. The Palaeoproterozoic Gallujavri Ultramafic Intrusion, Karasjok Greenstone Belt; Petrogenesis of a Trans-Crustal Magma System. J. Petrol. 63, 1–28. https://doi.org/10.1093/petrology/egac008.

Orvik, A.A., Slagstad, T., Sørensen, B.E., Millar, I., Hansen, H., 2022. Evolution of the Gállojávri ultramafic intrusion from U-Pb zircon ages and Rb-Sr, Sm-Nd and Lu-Hf isotope systematics. Precambr. Res. 379, 106813. https://doi.org/10.1016/j.precamres.2022.106813.

Paulsen, H.K., Bergh, S.G., Palinkaš, S.S., Karlsen, S.E., Kolsum, S., Rønningen, I.U., Armitage, P.E., Nasuti, A., 2021. Palaeoproterozoic foreland fold-thrust belt structures and lateral faults in the West Troms Basement Complex, northern Norway, and their relation to inverted metasedimentary sequences. Precambr. Res. 362, 106304. https://doi.org/10.1016/j.precamres.2021.106304.

Perello, J., Clifford, J.A., Creaser, R.A., Valencia, V.A., 2015. An example of synorogenic sediment-hosted copper mineralization: Geologic and geochronologic evidence from the Paleoproterozoic Nussir Deposit, Finnmark, Arctic Norway. Econ. Geol. 110, 677–689. https://doi.org/10.2113/econgeo.110.3.677.

Perttunen, V., Vaasjoki, M., 2001. U-Pb geochronology of the Peräpohja Schist Belt, northwestern Finland, in: Vaasjoki, M. (Ed.), Radiometric age determinations from Finnish Lapland and their bearing on the timing of Precambrian volcano-sedimentary sequences. Geological Survey of Finland. volume 33 of Special Paper, pp. 45–84. URL: http://tupa.gtk.fi/julkaisu/specialpaper/sp_033.pdf. 14 figures, 2 tables and 6 appendices.

Pharaoh, T.C., Ramsey, D., Jansen, Ø., 1983. Stratigraphy and structure of the northern part of the Repparfjord - Komagfjord window, Finnmark, Northern Norway. Norges Geologiske Undersøkelse Bulletin 377, 1–45. URL: https://www.ngu.no/FileArchive/NGUPublikasjoner/NGUnr_377_Bulletin_68.pdf.

Puchtel, I., Brügmann, G., Hofmann, A., Kulikov, V., Kulikova, V., 2001. Os isotope systematics of komatiitic basalts from the Vetreny belt, Baltic Shield: evidence for a chondritic source of the 2.45 Ga plume. Contrib. Miner. Petrol. 140, 588–599. https://doi.org/10.1007/s004100000203.

Puchtel, I.S., Arndt, N.T., Hofmann, A.W., Haase, K.M., Kröner, A., Kulikov, V.S., Kulikova, V.V., Garbe-Schönberg, C.D., Nemchin, A.A., 1998. Petrology of mafic lavas within the Onega plateau, central Karelia: evidence for 2.0 Ga plume-related continental crustal growth in the Baltic Shield. Contrib. Miner. Petrol. 130, 134–153. https://doi.org/10.1007/s004100050355.

Puchtel, I.S., Brügmann, G.E., Hofmann, A.W., 1999. Precise Re–Os mineral isochron and Pb–Nd–Os isotope systematics of a mafic–ultramafic sill in the 2.0 Ga Onega plateau (Baltic Shield). Earth Planet. Sci. Lett. 170, 447–461. https://doi.org/10.1016/s0012-821x(99)00118-1.

Puchtel, I.S., Haase, K.M., Hofmann, A.W., Chauvel, C., Kulikov, V.S., Garbe-Schönberg, C.D., Nemchin, A.A., 1997. Petrology and geochemistry of crustally contaminated komatiitic basalts from the Vetreny Belt, southeastern Baltic Shield: Evidence for an early Proterozoic mantle plume beneath rifted Archean continental lithosphere. Geochim. Cosmochim. Acta 61, 1205–1222. https://doi.org/10.1016/s0016-7037(96)00410-3.

Puchtel, I.S., Mundl-Petermeier, A., Horan, M., Hanski, E.J., Blichert-Toft, J., Walker, R. J., 2020. Ultra-depleted 2.05 Ga komatiites of Finnish Lapland: Products of grainy late accretion or core-mantle interaction? Chem. Geol. 554, 119801. https://doi.org/10.1016/j.chemgeo.2020.119801.

Rasmussen, B., Bekker, A., Fletcher, I.R., 2013. Correlation of Paleoproterozoic glaciations based on U-Pb zircon ages for tuff beds in the Transvaal and Huronian Supergroups. Earth Planet. Sci. Lett. 382, 173–180. https://doi.org/10.1016/j.epsl.2013.08.037.

Rastas, P., Huhma, H., Hanski, E., Lehtonen, M.I., Härkönen, I., Kortelainen, V., Mänttäri, I., Paakkola, J., 2001. U-Pb isotopic studieson the Kittilä greenstone area, central Lapland, Finland. In: Vaasjoki, M. (Ed.), Radiometric age determinations from Finnish Lapland and their bearing on the timing of Precambrian volcano-sedimentary sequences. Geological Survey of Finland, Special Paper, pp. 95–141. URL: https://pdfs.semanticscholar.org/e031/2d9df6c08386ad2f4764f8c8c3905bfe4a58.pdf.

Roberts, D., Davidsen, B., 2011. Bergrunnsgeologisk kart Lakselv 2035 III, m 1:50 000, revidert foreløpig utgave. Norges Geologiske Undersøkelse.

Roberts, H., Dahl, P., Kelley, S., Frei, R., 2002. New ^{207}Pb–^{206}Pb and ^{40}Ar–^{39}Ar ages from SW Montana, USA: constraints on the Proterozoic and Archean tectonic and depositional history of the Wyoming Province. Precambr. Res. 117, 119–143. https://doi.org/10.1016/s0301-9268(02)00076-1.

Räsänen, J., Huhma, H., 2001. U-Pb datings in the Sodankylä schist aea, central finnish lapland, in: Vaasjoki, M. (Ed.), Radiometric age determinations from Finnish Lapland and their bearing on the timing of Precambrian volcano-sedimentary sequences. Geological Survey of Finland. volume 33 of Special Paper, pp. 153–188. URL: http://tupa.gtk.fi/julkaisu/specialpaper/sp_033.pdf. 19 figures, 2 tables and one appendix.

Satish-Kumar, M., Shirakawa, M., Imura, A., Otsuji-Makino, N., Imanaka-Nohara, R., Malaviarachchi, S., Fitzsimons, I., Sajeev, K., Grantham, G., Windley, B., Hokada, T., Takahashi, T., Shimoda, G., Goto, K., 2021. A geochemical and isotopic perspective on tectonic setting and depositional environment of Precambrian meta-carbonate rocks in collisional orogenic belts. Gondwana Res. 96, 163–204. https://doi.org/10.1016/j.gr.2021.03.013.

Sharkov, E.V., Smolkin, V.F., 1997. The early Proterozoic Pechenga-Varzuga Belt: a case of Precambrian back-arc spreading. Precambr. Res. 82, 133–151. https://doi.org/10.1016/s0301-9268(96)00041-1.

Siedlecka, A., 1985. Geology of the Iešjav'ri - Skoganvarre area, northern Finnmarksvidda, North Norway. Norges Geologiske Undersøkelse Bulletin 403, 103–112. URL: https://hdl.handle.net/11250/2674241.

Siedlecka, A., Davidsen, B., Rice, A.H.N., Townsend, C., 2011. Bergrunnsgeologisk kart Skoganvarre 2034 IV, m 1:50 000, revidert foreløpig utgave. Norges Geologiske Undersøkelse.

Siedlecka, A., Iversen, E., Krill, A.G., Lieungh, B., Often, M., Sandstad, J.S., Solli, A., 1985. Lithostratigraphy and correlation of theArchean and Early Proterozoic rocks of Finnmarksvidda and the Sørvaranger district. Norges Geologiske Undersøkelse Bulletin 403, 7–36. URL: https://hdl.handle.net/11250/2674240.

Skuf'in, P., Theart, H., 2005. Geochemical and tectono-magmatic evolution of the volcano-sedimentary rocks of Pechenga and other greenstone fragments within the Kola Greenstone Belt, Russia. Precambr. Res. 141, 1–48. https://doi.org/10.1016/j.precamres.2005.07.004.

Skuf'in, P.K., Bayanova, T.B., 2006. Early Proterozoic central-type volcano in the Pechenga structure and its relation to the ore-bearing gabbro-wehrlite complex of the Kola Peninsula. Petrology 14, 609–627. https://doi.org/10.1134/s0869591106060063.

Skyttä, P., Piippo, S., Kloppenburg, A., Corti, G., 2019. 2.45 Ga break-up of the Archaean continent in Northern Fennoscandia: Rifting dynamics and the role of inherited structures within the Archaean basement. Precambr. Res. 324, 303–323. https://doi.org/10.1016/j.precamres.2019.02.004.

Slagstad, T., Willemoes-Wissing, B., Coint, N., Stampolidis, A., Ganerød, M., Ofstad, F., 2015. Geology and metallogenic potential of the northwesternmost Norrbotten Province around Altevatn in Troms, northern Norway. Norw. J. Geol. 95, 445–466 doi:http:/dx.doi.org/10/17850/njg95-3-07.

Solli, A., 1983. Precambrian stratigraphy in the Masi area, southwestern Finnmark, Norway. Norges Geologiske Undersøkelse Bulletin 380, 97–105. URL: https://www.ngu.no/FileArchive/NGUPublikasjoner/NGUnr_380_Bulletin_70_Solli_97_105.pdf.

Stepanova, A., Stepanov, V., 2010. Paleoproterozoic mafic dyke swarms of the Belomorian Province, eastern Fennoscandian Shield. Precambr. Res. 183, 602–616. https://doi.org/10.1016/j.precamres.2010.08.016.

Stepanova, A.V., Salnikova, E.B., Samsonov, A.V., Egorova, S.V., Larionova, Y.O., Stepanov, V.S., 2015. The 2.31 Ga mafic dykes in the Karelian Craton, eastern Fennoscandian shield: U-Pb age, source characteristics and implications for continental break-up processes. Precambr. Res. 259, 43–57. https://doi.org/10.1016/j.precamres.2014.10.002.

Stepanova, A.V., Samsonov, A.V., Salnikova, E.B., Puchtel, I.S., Larionova, Y.O., Larionov, A.N., Stepanov, V.S., Shapovalov, Y.B., Egorova, S.V., 2014. Palaeoproterozoic continental MORB-type tholeiites in the Karelian craton: Petrology, geochronology, and tectonic setting. J. Petrol. 55, 1719–1751. https://doi.org/10.1093/petrology/egu039.

Stokmo, E.B., 2020. Superimposed macro- and mesoscale folds, and their relation to ductile shear zones in the Karasjok Greenstone Belt, Finnmark. UiT The Arctic University of Norway, Department of Geosciences, Norway. mathesis. URL: https://hdl.handle.net/10037/18575.

Söderlund, U., Hofmann, A., Klausen, M.B., Olsson, J.R., Ernst, R.E., Persson, P.O., 2010. Towards a complete magmatic barcode for the Zimbabwe craton: Baddeleyite U-Pb dating of regional dolerite dyke swarms and sill complexes. Precambr. Res. 183, 388–398. https://doi.org/10.1016/j.precamres.2009.11.001.

Torgersen, E., Viola, G., Sandstad, J.S., 2015. Revised structure and stratigraphy of the northwestern Repparfjord Tectonic Window, northern Norway. Norw. J. Geol. 95, 397–421. https://doi.org/10.17850/njg95-3-06.

Torske, T., Bergh, S.G., 2004. The Čaravarri Formation of the Kaukokeino Greenstone Belt, Finnmark, North Norway: a Palaeoproterozoic foreland basin succession. Norges Geologiske Undersøkelse Bulletin 442, 5–22. URL: http://www.ngu.no/upload/Publikasjoner/Bulletin/Bulletin442_5-22.pdf.

Valley, J.W., 1986. Stable isotope geochemistry of metamorphic rocks, in: Valley, J.W., Taylor, H.P., O'Neil, J.R. (Eds.), Stable Isotopes in High Temperature Geological Processes. De Gruyter. volume 16 of Reviews in Mineralogy. chapter 13, pp. 445–490. doi:10.1515/9781501508936-018.

Valley, J.W., 2001. Stable isotope thermometry at high temperatures. Rev. Mineral. Geochem. 43, 365–413. https://doi.org/10.2138/gsrmg.43.1.365.

Vogel, D.C., Vuollo, J.I., Alapieti, T.T., James, R.S., 1998. Tectonic, stratigraphic, and geochemical comparisons between ca. 2500–2440 Ma mafic igneous events in the Canadian and Fennoscandian Shields. Precambr. Res. 92, 89–116. https://doi.org/10.1016/s0301-9268(98)00073-4.

Vrevsky, A.B., 2011. Petrology, age, and polychronous sources of the initial magmatism of the Imandra-Varzuga paleorift, Fennoscandian shield. Petrology 19, 521–547. https://doi.org/10.1134/s0869591111050067.

Vuollo, J., Huhma, H., 2005. Paleoproterozoic mafic dikes in NE Finland, in: Lehtinen, M., Nurmi, P.A., Rämö, O.T. (Eds.), Precambrian Geology of Finland — Key to the Evolution of the Fennoscandian Shield. Elsevier. volume 14 of Developments in Precambrian Geology. chapter 5, pp. 195–236. doi:10.1016/s0166-2635(05)80006-4.

Yang, S.H., Hanski, E., Li, C., Maier, W.D., Huhma, H., Mokrushin, A.V., Latypov, R., Lahaye, Y., O'Brien, H., Qu, W.J., 2016. Mantle source of the 2.44–2.50 Ga mantle plume-related magmatism in the Fennoscandian Shield: evidence from Os, Nd, and

Sr isotope compositions of the Monchepluton and Kemi intrusions. Miner. Deposita 51, 1055–1073. https://doi.org/10.1007/s00126-016-0673-9.
Zakharov, V., Lubnina, N., Stepanova, A., Gerya, T., 2022. Simultaneous intruding of mafic and felsic magmas into the extending continental crust caused by mantle plume underplating: 2D magmatic-thermomechanical modeling and implications for the Paleoproterozoic Karelian Craton. Tectonophysics 822, 229173. https://doi.org/10.1016/j.tecto.2021.229173.
Zwaan, K.B., Gauthier, A.M., 1980. Alta og Gargia. beskrivelse til de berggrunnsgeologiske kart 1834 I og 1934 IV - M 1: 50 000. Norges geologiske undersøkelse Skrifter 32, 1–47. URL: https://hdl.handle.net/11250/2675088. (In Norwegian with English abstract).